Received: 1 December 2021 | Revised: 10 March 2022 | Accepted: 22 March 2022

DOI: 10.1002/esp.5369

RESEARCH ARTICLE

ESPL WILEY

How debris-flow composition affects bed erosion quantity and mechanisms: An experimental assessment

Lonneke Roelofs | Pauline Colucci | Tjalling de Haas

Department of Physical Geography, Faculty of Geosciences, Utrecht University, Utrecht, The Netherlands

Correspondence
Lonneke Roelofs, Department of Physical Geography, Faculty of Geosciences, Utrecht University, Princetonlaan 8a, 3584 CB Utrecht, The Netherlands.
Email: l.roelofs@uu.nl

Funding information
Netherlands Organisation for Scientific Research (NWO), Grant/Award Numbers: 0.16.Veni.192.001, OCENW.KLEIN.495

Abstract

Understanding erosion and entrainment of material by debris flows is essential for predicting and modelling debris-flow volume growth and hazard potential. Recent advances in field, laboratory and modelling studies have distilled two driving forces behind debris-flow erosion: impact and shear forces. How erosion and these forces depend on debris-flow composition and interact remains unclear. Here, we experimentally investigate the effects of debris-flow composition and volume on erosion processes in a small-scale flume with a loosely packed bed. We quantify the effects of gravel, clay and solid fraction in the debris flow on bed erosion. Erosion increased linearly with gravel fraction and volume, and decreased with increasing solid fraction. Erosion was maximal around a volumetric clay fraction of 0.075 (fraction of the total solid volume). Under varying gravel fractions and flow volumes erosion was positively related to both impact and shear forces, while these forces themselves are also correlated. Results further show that internal dynamics driving the debris flows, quantified by Bagnold and Savage numbers, correlate with erosional processes and quantity. Impact forces became increasingly important for bed erosion with increasing grain size. The experiments with varying clay and solid fractions showed that the abundance and viscosity of the interstitial fluid affect debris-flow dynamics, erosional mechanisms and erosion magnitude. High viscosity of the interstitial fluid inhibits the mobility of the debris flow, the movement of the individual grains and the transfer of momentum to the bed by impacts, and therefore inhibits erosion. High solid content possibly decreases the pore pressures in the debris flow and the transport capacity, inhibiting erosion, despite high shear stresses and impact forces. Our results show that bed erosion quantities and mechanisms may vary between debris flows with contrasting composition, and stress that entrainment models and volume-growth predictions may be substantially improved by including compositional effects.

KEYWORDS
debris flow, erosion, entrainment, impact force, basal-shear force, experiments

1 | INTRODUCTION

Debris flows are fast-moving masses of soil, rock and fluid that occur in mountainous regions (e.g., Costa, 1984; Iverson, 1997). Their composition varies greatly, but debris flows typically consist of a coarse-grained front followed by a finer-grained body (Hungr, 1999; Iverson, 1997; McArdell et al., 2007; Pierson, 1986; Takahashi, 1981). When flowing down mountainsides and through valleys, debris flows can grow in volume due to entrainment of bed material by eroding the underlying bed, which can be bedrock and/or unconsolidated substrate. At locations with an abundance of loose substrate, volume growth can be up to several orders of magnitude (De Haas &

Woerkom, 2016; Frank et al., 2015; Hungr et al., 2005; Navratil et al., 2013; Reid et al.2016; Santi et al., 2008; Simoni et al., 2020; Takahashi, 1981). If debris flows grow in size their destructive power increases and so does their hazard to mountain communities (Dowling & Santi, 2014; Rickenmann, 1999, 2005). The erodible power of debris flows, combined with consecutive flow activity, is further suggested to be a primary process in cutting valleys in steep landscapes (Stock & Dietrich, 2003, 2006). On a shorter timescale, the erosion, reworking and deposition of sediment by debris flows is a main driver in the evolution of alluvial and debris-flow fans (Beaty, 1963; Blair & McPherson, 1994; De Haas et al., 2014). To minimize debris-flow hazards on Earth and decipher their ability to change landscapes we aim to gain a better understanding of the mechanisms of debris-flow erosion and the parameters that affect it.

Observations from field and experimental studies suggest two driving forces behind debris-flow erosion: (1) basal-shear forces; sliding of the flow along the bed (Frank et al., 2015; Hungr et al., 2005; Mangeney et al., 2007; Takahashi, 1978, 1981); and (2) impact forces; collisions between the grains and the bed (Berger et al., 2011; Hsu et al., 2008; Stock & Dietrich, 2006). Basal-shear force is dependent on the bulk density of the flow, flow thickness, gravity and the slope (e.g., De Haas & Woerkom, 2016). Particle impacts on the bed cause fluctuating basal forces and high-frequency seismic signals (Farin et al., 2019). These impact forces are the direct product of particle diameter and the granular temperature, that is, the velocity fluctuation of the particles relative to the velocity of the flowing mass (Berger et al., 2011; Farin et al.2019; Hsu et al., 2008; Stock & Dietrich, 2006). The magnitude of impact forces is further influenced by debris-flow velocity, flow depth and the velocity structure in the flow (Farin et al., 2019). A third factor influencing the (relative) importance of either two forces is the abundance and viscosity of the interstitial fluid. High abundance and viscosity have been hypothesized to lead to high pore-fluid pressure, which buffers grain interactions and inhibits particle segregation, thus decreasing impact forces (Bagnold, 1954; De Haas et al., 2015; Hsu et al.2008; Iverson, 1997; Iverson et al., 2010; Kaitna et al., 2016; Major, 2000; Major & Iverson, 1999; McCoy et al., 2010; Vallance & Savage, 2000). Others have, however, suggested that as muddy matrices are able to mobilize and transport larger clasts, an increased viscosity of the interstitial fluid may increase impact forces (Hsu et al., 2014). Iverson et al. (2011) showed, by means of large-scale experiments, that besides the abundance of interstitial fluid of the debris flow itself, bed wetness strongly affects erosion. An increase in bed wetness allows for larger positive pore pressures when overridden by a debris flow (also observed by McCoy et al.2012), which increases flow momentum and speed, facilitating progressive erosion of the bed. High pore pressures, and thus a large water content, also increase entrainment by reducing grain-to-grain basal friction (e.g., Iverson et al., 2011; Li et al., 2020), and at the same time favouring undrained loading and liquefaction (e.g., Hungr et al., 2005; Sassa & hui Wang, 2005).

The importance of entrainment and erosion for debris-flow volume and hazard has led to the development of multiple entrainment models (e.g., Abancó & Hürlimann, 2014; Baggio et al., 2021; Frank et al.2015; Han et al., 2016; Hungr et al., 2005; Iverson, 2012; Iverson & Ouyang, 2015; Li et al., 2020; Ouyang et al., 2015; Takahashi, 1978). These entrainment and erosion models have different approaches, varying from empirical (e.g., Baggio et al., 2021; Dietrich & Krautblatter, 2019; Frank et al., 2015) to analytical (e.g., Iverson, 2012; Iverson & Ouyang, 2015; Pudasaini & Fischer, 2020). As Kang and Chan (2018) summarized, the models using an analytical approach use governing equations based on the mechanics of the erosion process, often using shear, whereas in the empirical approach erosion correlates with the kinematic characteristics of the flow such as flow velocity and shear stress. The entrainment models with empirical elements are often coupled to depth-integrated debris-flow models by calibrating erosion rates, maximum erosion depths, erosion coefficients and/or other empirical constants to field data (Armanini et al., 2009; Baggio et al., 2021; Dietrich & Krautblatter, 2019; Frank et al., 2015, 2017; Gregoretti et al., 2019). In addition, some use an equilibrium volumetric sediment concentration to predict whether the debris flow can incorporate and entrain material (e.g., Armanini et al., 2009; Chen & Zhang, 2015) or use a critical flow depth above which erosion occurs (Han et al.2016). Many analytical and empirical models consider erosion as a function of shear forces, but how momentum conservation is incorporated differs greatly (Iverson & Ouyang, 2015). Despite the ability of both empirical and analytical models to predict erosion and entrainment relatively well in specific debris-flow torrents, the need for parameter calibration and the ongoing discussions about analytical models (see, e.g., Iverson & Ouyang, 2015; Kang & Chan, 2018; Pudasaini & Fischer, 2020) indicates the need for a better understanding of debris-flow erosional processes.

Field and laboratory studies have shed light on the possible importance of impact forces on erosion, which is currently not directly incorporated in the earlier discussed models. A field study by Berger et al. (2011) demonstrated that erosion and entrainment of loose material in the Illgraben torrent were associated with the impact of the coarse-grained flow front on the channel bed. They observed erosion before maximum values for flow depth, total normal stress and shear stress, but during the period of largest pressure fluctuations, which are caused by particle collisions with the bed. In contrast to Berger et al. (2011), the study by McCoy et al. (2013) could not find a difference in force fluctuation distribution between granular surges and the more watery intersurge flows. In addition to this contrasting observation, McCoy et al. (2012) could not find a direct link between the magnitude of pressure fluctuations and erosion. They still hypothesized, however, that high-frequency stress fluctuations might facilitate entrainment. Experimental results from a rotating drum show that bedrock erosion increases when inertial stresses, caused by impacts, increase in both dry and wet granular flows (Hsu et al., 2008), and that a larger representative grain size correlates with more erosion (Hsu et al., 2008, 2014). Other studies on impacts endorse the correlation between the magnitude of impact forces and particle diameter (De Haas et al., 2021; Farin et al., 2019; He et al., 2016). However, in the field study by Berger et al. (2011), the link between grain size and erosion could not be distilled as grain size was not recorded and only two debris flows from the same torrent were studied. It can, however, be hypothesized that as the largest clasts occurred at the front of the flow, grain size did affect the inertial stresses. To our knowledge, the effect of inertial stresses, linked to grain size, on the erosion of a loose substrate has not yet been studied directly.

The largely unknown influence of, and interaction between, shear and impact forces on debris-flow erosion suggest that certain

boundary conditions, such as flow and bed composition and flow volume, could be affecting erosion and erosional mechanisms. Flow and bed composition are especially difficult to assess in the field (Iverson, 1997; Major & Voight, 1986). The few field studies looking at the influence of flow composition on debris flow dynamics, however, show that the grain composition directly links to debris flow properties (Li et al., 2015; Wang et al.2018) and velocity (Liu et al., 2020). In experiments, the impact of debris flow composition on debris flow dynamics, run-out distance and deposit morphology has been studied (De Haas et al., 2015). De Haas et al. (2015) found that run-out increases with increasing water and clay fractions and that there is an optimum run-out distance when increasing gravel content. Initially, increasing gravel content increases flow velocity and run-out distance, but increasing gravel further decreases flow velocity and run-out distance. They explained their findings as being the result of the interaction between grain collisional forces, pore-fluid pressure and diffusivity. In addition, rheometric investigations have shown that the behaviour of debris-flow mixtures varied with the concentration of solids, grain-size distributions and ultimately shear rate (Jeong, 2010; Major & Pierson, 1992; O'Brien & Julien, 1988; Phillips & Davies, 1991; Scotto di Santolo et al., 2010). Based on these findings we hypothesize that debris-flow composition will also influence debris-flow erosion and erosional mechanisms—a hypothesis underlined by the work of De Haas and Woerkom (2016). They showed that in experimental debris flows an increase in the water fraction and grain size of the debris flow resulted in an increase in basal-scour depth, and increasing clay content resulted in a decrease in the scour depth—a correlation which they coupled to the dependence of erosion on basal-shear stress. The only exception to this conclusion was their observation on experiments with a very large gravel content, which lacked the relation between basal-shear and erosion. They hypothesized that during these experiments collisional stresses had a relatively large influence on the flow dynamics. Their set-up, however, did not allow for conclusive statements on this. The small-scale flume set-up, with a small grain size relative to flow depth, resulted in an overall small influence of grain collisional stresses, which is in contrast to observations from the field (Berger et al.2011).

Field studies further reveal that maximum flow depth is an important control on the pattern and magnitude of erosion (Schürch et al., 2011), that debris-flow magnitude relates to the balance between erosion and deposition (Chen & Zhang, 2015), and that entrainment is correlated with terrain slope (Baggio et al., 2021; Gregoretti et al., 2019; Reid et al., 2016; Simoni et al., 2020; Theule et al., 2015). Nonetheless, the scatter and uncertainties in these field studies are large and the relations that are found do not provide a process-based explanation of debris-flow erosion. A complicating factor in studying erosion processes in the field, which could explain some of the observed scatter, is the influence and often chaotic nature of the debris flow initiation mechanism, landsliding and other slope failures or grain-by-grain bulking. When landsliding or slope failures trigger debris flows, initial sediment concentration is high, which may limit erosion. In contrast, when grain-by-grain bulking initiates debris flows, erosion starts under the influence of water-dominated flows before transitioning into a debris flow (McGuire et al., 2017), thereby allowing entrainment of large amounts of sediment.

To summarize, there is no consensus on the exact processes and parameters controlling debris-flow erosion. Both impact forces, shear forces and the interaction between the fluid and solid phase in a debris flow likely affect erosion. How these forces and their interactions are affected by boundary conditions, such as debris-flow composition and flow volume, is not well understood. In addition, we need to understand the forces dominating erosion in contrasting flows (e.g., granular vs. viscous) to effectively predict and model debris-flow erosion as a function of their composition.

The objective of our study is to unravel the effects of debris-flow composition on debris-flow erosion and erosional mechanisms. We aim at understanding the mechanisms of debris-flow erosion under different debris-flow compositions, and aim to assess the erosion potential as a function of composition. As correctly assessing debris flow composition in the field has been proven almost impossible (Iverson, 1997; Major & Voight, 1986), and spatiotemporal patterns of erosion in debris flow torrents are highly variable, dynamic and possibly affected by check dams (De Haas et al., 2020), we use experiments in a small-scale debris-flow flume to answer these questions. Experiments allow for complete control over the debris-flow composition, volume and slope, and provide us the opportunity to test a wide variety of flow compositions and debris-flow volumes. As volume growth in debris flows overriding unconsolidated substrate is the largest, we focus our effort on the erosion of an unconsolidated bed.

2 | MATERIALS AND METHODS

To study the effects of debris-flow composition on debris-flow erosion and erosional mechanisms, we conducted a series of experiments in a flume of 5.4 m long and 0.3 m wide with an erodible, unsaturated and loosely packed, unconsolidated bed. The flume set-up used was similar to the set-up presented in De Haas et al. (2021). For our experiments the set-up from De Haas et al. (2021) has been expanded with an erodible bed (see Figure 1). In our experiments we systematically varied the composition of the debris flow while keeping the composition of the bed constant. The debris-flow mixture consisted of four components in varying fractions: gravel, sand, clay (kaolinite) and water. The erodible bed consisted of sand (98% of solid fraction), kaolinite clay (2% of solid fraction) and water (11% of total weight). The composition of the bed was selected based on preliminary tests in the flume aimed at finding a balance between enabling erosion and not fully removing the bed. We tested the effects of the gravel and clay fractions in the flow, as well as the total solid fraction, including gravel, sand and clay, and the total volume of the debris flow. When increasing the gravel and clay fraction the total solid fraction was kept constant, meaning that the fraction of the other solids was decreased proportionally. Under varying total solid fractions, the relative percentages of gravel, sand and clay were kept constant, but the ratio of solids to water changed. When varying flow volume the composition of the debris flow was kept constant. The intended purpose of the experiments with varying flow volume was to establish the significance of debris-flow composition on erosion relative to the size and flow depth of a debris flow, since we already know from field studies that debris flow size and depth are important controls on erosion magnitude (Chen & Zhang, 2015; Schürch et al.2011). In total, 96 experiments were executed, of which 73 had a flume inclination of 34° (see Supporting Information Table 1). The angle of the flume is steep, but corresponds to the upper reach of debris-flow channels

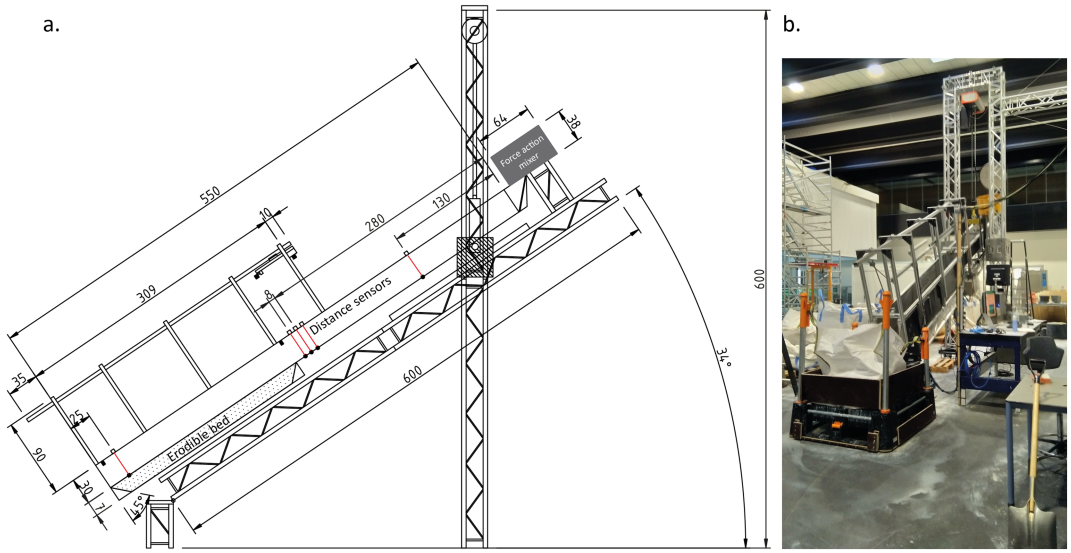

FIGURE 1 Schematic (a) and photo (b) of the flume. Sketch: grey rectangle represents the force action mixer and the dotted trapezoid represents the erodible bed. All dimensions are in centimetres [Color figure can be viewed at wileyonlinelibrary.com]

dominated by erosion (Rengers et al., 2021; Simoni et al.2020). In addition, because our experimental flows are relatively small in volume and flow depth, we need a large angle for increasing shear stress and flow velocity with the purpose of scaling erosion magnitude. Based on the outcome of the experiments at 34°, key experiments were selected and performed again on 32° and 30°, to test the effects of the flume angle. To account for the effects of natural variability, each experimental setting at a flume angle of 34° was repeated twice. The experiments performed with lower flume angles were performed once. When during or after the experiment the erodible bed in the flume slumped, for reasons unrelated to the passing of the debris flows, the results were discarded and the experiment was repeated.

2.1 | Experimental set-up and data analyses

The flume consists of a straight, rectangular channel of 0.3 m wide and 5.4 m long, a mixing tank with a forced-action mixer (Baron E120) and a custom-made release gate (Figure 1). The flume was tilted at the beginning of every experiment. Mixing of the sediment and water took place for 30 s, during the lifting procedure, and stopped 0.8 s before the gate opened. Our set-up thus differs from earlier experiments on debris flow erosion by Lanzoni et al. (2017), who focused on the influence of the triggering run-off. Our experimental set-up enables us to study debris flow erosion mechanisms and potential of different compositions and volumes independent of the duration and/or volume of the triggering run-off. This provides insights into debris flow erodible mechanisms and potential, beyond the often smaller natural variations in debris flow composition.

In the lower half of the flume the bottom was lowered by 7 cm to create space for an erodible bed with a length of 2.5 m. Along the entire length of the flume the floor was covered with sandpaper to simulate natural channel roughness.

Along the length of the flume five distance sensors were installed (locations are indicated by red lines in Figure 1). Two Baumer OADM 20U2480/S14C distance sensors (at 2.9 and 2.98 m), which are capable of measuring at sub-millimetre accuracy, and three Baumer FADK14U4470/S14/IO distance sensors (at 1.4, 2.81 and 5.36 m), which measure at 1–2 mm accuracy. With the data from these sensors, flow depth along the flume was recorded during the experiments and flow velocities were inferred from the arrival time of the flow front.

In the middle of the flume, just upstream of the erodible bed, a measurement plate was installed at 2.98 m connecting to a Geospace GS-20DX geophone, which records seismic ground vibrations. The geophone records seismic vibrations in both vertical and horizontal directions and has a natural frequency of 10 Hz and a flat response to 1000 Hz. To minimize seismic vibrations unrelated to the debris flow, the outside of the flume was covered by anti-drumming material (Vibraflex UF 35 mm). Despite this anti-drumming material, a 2.5–50 Hz band-stop filter was applied to the seismic and normal-force data to filter out the low-frequency vibrations caused by the mixing tank (De Haas et al., 2021; Hsu et al., 2014). For data reduction purposes, we used the mean of the absolute values of the filtered geophone signal over a 0.05 s time window for analyses (De Haas et al., 2021). All sensors in the flume sampled slope-normal at a frequency of 9500 Hz and continued sampling for a duration of 30 s after the opening of the gate. After these 30 s the flume was lowered again, reaching a horizontal position.

Erosion of and deposition on top of the erodible bed were captured with a Vialux z-Snapper 3-D scanner, which created a 3-D point cloud with sub-millimetre accuracy from a fringe pattern projector and camera (Hoefling, 2004). A scan of the bed was made before each experiment and after the debris flow had passed. The point clouds were denoised with MATLAB to remove outliers before they were transformed to gridded digital elevation models (DEMs) of 0.3 mm resolution by the use of natural neighbour interpolation. DEM of differences (DoD) was used to quantify erosion and deposition volumes and patterns. To further capture debris flow dynamics and behaviour during the experiments, two GoPro HERO6 cameras were placed above the flume and at the downstream end of the channel. The videos were shot at 1040 dpi at 60 frames per second.

TABLE 1 Varied debris flow characteristics and channel slopes

Parameter	Unit	Reference	Range
Gravel fraction	kg	9.6	0–28.8
	Volume fraction (of solids)	0.2	0–0.6
	Weight fraction (of total df)	0.16	0–0.48
Clay fraction	kg	2.4	0–9.6
	Volume fraction (of solids)	0.05	0–0.2
	Weight fraction (of total df)	0.04	0–0.16
Solid fraction	kg	48	40–53.33
	Volume fraction (of total df)	0.6	0.43–0.75
	Weight fraction (of total df)	0.2	0.11–0.33
Flow volume	m^3	0.03	0.018–0.054
	kg	60	36–108
Channel slope	Degrees	34	30, 32, 34

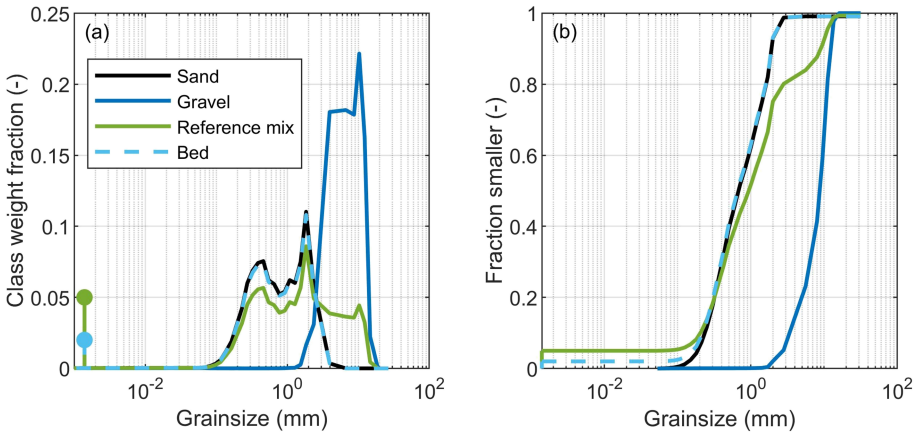

FIGURE 2 Grain size distribution of the bed sediment and debris flow mixtures: (a) frequency distribution; (b) cumulative particle-size distribution. Note that the reference mixture refers to the reference debris flow mix [Color figure can be viewed at wileyonlinelibrary.com]

2.2 | Debris flow and bed composition

As discussed above our debris flows were composed of clay (kaolin), sand, angular gravel and water. Our reference experiment had a total mass of 60 kg (0.03 m^3), of which 12 kg consisted of water. The sediment mixture of the reference experiment volumetrically comprised 20% gravel (2–16 mm), 75% sand (0.09–2 mm) and 5% clay (~ 2 μ m) (similar to De Haas & Woerkom, 2016; De Haas et al., 2015, 2021). We systematically varied the gravel as a fraction of the total weight from 0 to 0.6 and the clay from 0 and 0.2. We varied the total solid fraction as a fraction of the total volume from 0.43 to 0.75 and the flow mass of the debris flow from 36 to 108 kg (0.018–0.054 m^3) (see Table 1 and Supporting Information Table 1. The grain size distributions of the sand and gravel, and the combined distribution for the reference debris flow, can be found in Figure 2.

The erodible bed was composed of clay (kaolin), sand and water. For every experiment ~ 90 kg of mixture was prepared for the bed. This was more than fitted in the bed but made filling and levelling the bed easier. Of this mixture, 89% of the weight consisted of solids and 11% of water. Of the solid fraction, 98% of the weight consisted of sand and 2% consisted of clay. The contents of the bed were thoroughly mixed with a hand-held forced action mixer before being emplaced in the flume. A trowel was used to level the bed at a constant height and replicate the same loose packing in the bed for every experiment. To ascertain that the wetness of the levelled bed was constant, we measured and registered the moisture content of the bed for every run at 12 locations along the length of the flume with an HH2 Moisture Meter and ML3 ThetaProbe (soil moisture accuracy 1%) (see Supporting Information Table 1).

2.3 | Characterization of flow characteristics

Basal-shear stress, momentum and seismic energy are used to quantify the forces on the bed. Peak basal shear stress is estimated from simple flow metrics:

$$\tau = \rho g H \sin S, \quad (1)$$

where ρ is the density of the flow (kg/m^3), g is gravitational acceleration (m/s^2), H is maximum flow depth (m) just before the erodible bed and S is the channel-bed slope. We approximate flow density as bulk density when perfectly mixed and use maximum flow depth as input for depth. These assumptions introduce small deviations from reality as the flow front generally contains a relatively high solid fraction. The momentum of the flow is defined and calculated as

$$M = mu, \quad (2)$$

where m is the mass of the debris flow (kg) and u is the debris flow frontal velocity (m/s) just before the erodible bed. Frontal velocity is calculated by using the time until arrival of the flow front at the laser

distance sensor at 290 cm, just before the erodible bed. Seismic energy, a measure to quantify the cumulative impact force during the flow, was calculated as the integral of the squared amplitude of the vertical ground velocity of the entire flow (for further details on this procedure see De Haas et al., 2021; Schimmel et al., 2021). Note that shear force, momentum and seismic energy are all recorded and calculated just before the erodible bed. The values therefore represent the conditions in and underneath the debris flow before erosion could occur.

To characterize the dynamics in different flows and objectively compare them, three dimensionless numbers are used: the Bagnold, Savage and friction numbers. These numbers describe the relationship between the forces resisting motion in debris flows: collisional, frictional and viscous forces (Iverson, 1997; Iverson et al., 2010; Parsons et al., 2001). However, as we hypothesize these forces to affect debris-flow erosion, we will use these numbers as indicators for studying the relative importance of these three forces in the erosion process. The Bagnold number defines the ratio between collisional and viscous forces:

$$N_b = \frac{v_s \rho_s \delta^2 \gamma}{v_f \mu}, \quad (3)$$

where δ is the mean grain size of a debris flow mixture (m) (Iverson, 1997), v_s is the volumetric solids fraction and γ is the flow shear rate ($1/s$):

$$\gamma = \frac{\mu}{H}, \quad (4)$$

where μ is the interstitial fluid viscosity, which we estimate as (De Haas et al., 2015; Iverson, 1997; Thomas, 1965):

$$\frac{\mu}{\mu_w} = 1 + 2.5 v_{fines} + 10.05 {v_{fines}}^2 + 0.00273^{16.6 v_{fines}}, \quad (5)$$

where μ_w is the dynamic viscosity of pure water (equal to 0.001002 Pa s). According to Iverson (1997), collisional forces dominate at $N_b > 200$. The Savage number describes the ratio between collisional to frictional forces:

$$N_s = \frac{\rho_s \delta^2 \gamma^2}{(\rho_s - \rho_f) g H \tan\phi}, \quad (6)$$

where ϕ is the internal angle of friction, assumed to be 42° (De Haas et al., 2015; Parsons et al., 2001). For $N_s > 0.1$ collisional forces dominate viscous forces (Iverson, 1997). Lastly, the ratio of frictional to viscous forces is described as follows:

$$N_f = \frac{v_s (\rho_s - \rho_f) g H \tan\phi}{(1 - v_s) \gamma u}. \quad (7)$$

For $N_f > 2000$ frictional forces dominate over viscous forces according to cohesionless dry flows from Iverson (1997), but experimental data of wet experimental debris flows of Parsons et al. (2001) and De Haas et al. (2015) suggest that this transition already happens at $N_f > 100$ for the flow body and $N_f > 250$ for the flow front.

2.4 | Scale effects

Iverson (1997), Iverson and Denlinger (2001) and Iverson et al. (2010) have argued that small-scale debris-flow experiments suffer from scale effects that influence flow dynamics. They show that small-scale flows experience large effects of yield strength, viscous flow resistance and grain inertia compared to field size debris flows. In addition, they are insufficiently affected by pore-fluid pressure. However, the dimensionless numbers describing flow dynamics and forces within the debris flow in our flume are in the range of debris flows in the large-scale US Geological Survey flume and natural debris flows (Iverson, 1997), with Bagnold numbers between 81 and 2704, Savage numbers between 0.005 and 0.15, and friction numbers between 481 and 4757 (see Figure 4). This suggests that we are able to scale the forces and mechanisms controlling debris flow dynamics. By varying debris flow composition and volume we are then able to study the effects of different erosional processes and mechanisms on erosion in the lab, and by studying the dimensionless numbers describing our experimental flows we are able to find implications for the field. Furthermore, previous studies have shown that flow patterns and deposits as well as scaling relationships of experimental debris flows resemble those of natural debris flows (De Haas & Woerkom, 2016; De Haas et al., 2015; Paola et al., 2009). We emphasize that the experiments presented here are not intended as 1:1 scaled analogues, but rather aim at examining the interaction between shear and impact forces in the debris-flow erosion process. The general trends and differences between experiments, rather than the detailed results of a single experiment, are of primary interest to this work.

3 | RESULTS

3.1 | Flow behaviour and regime

The experimental debris flows followed a similar flow pattern, regardless of their composition or volume. The debris flows came down in one or two surges. In the case of two surges, an initial flow front formed upstream that was overtaken by a subsequent surge just before or after arriving at the erodible bed. In all experiments gravel concentration was higher at the flow front and saltating and rolling gravel outran the main flow front (akin to De Haas et al., 2021, with a similar set-up). When the gravel content of the debris flow increased, the volume of gravel outrunning the debris flow also increased.

In all experiments, flow depth was highest at the debris-flow front (see Figure 3a for an example). Depth increased quickly when the flow front arrived and decreased gradually when the flow front passed. The largest seismic vibrations were recorded underneath the flow front (see Figure 3b,c for an example) and the magnitude of the seismic signal decreased more quickly than the flow depth.

Frictional forces dominated in the majority of our experimental debris flows. In almost all experiments Bagnold numbers indicated that collisional forces dominated over viscous forces (Figure 4a–d), and Savage numbers showed that frictional forces dominated over collisional forces (Figure 4e–h). Only in experiments with a very high clay (volume fraction > 0.15) or low solid content (volume fraction < 0.55) did viscous forces dominate over collisional forces (Figure 4b,c)

and only in experiments with a volumetric gravel fraction > 0.4 did collisional forces dominate over frictional forces (Figure 4e).

3.2 | Flow characteristics as a function of debris-flow composition and volume

The maximum flow velocity of the debris flows before flowing onto the erodible bed ranged between 1.5 and 2.5 m/s and maximum flow depth between 2.5 and 7 cm (Figure 5a–h). Maximum flow velocities under smaller flume angles decreased slightly, whereas flow depth increased slightly. Maximum flow velocity decreased slightly when gravel fraction increased (Figure 5a) and increased slightly when flow volume increased (Figure 5d). When increasing the fraction of clay in the debris flow, maximum flow velocity is reached at a volumetric clay content of 0.075–0.1 (Figure 5b). At lower and higher clay contents the maximum flow velocity is smaller. Flow velocity is similar for the experiments with a varying fraction of solids (Figure 5c).

Increasing gravel fraction or flow volume results in larger maximum flow depths. For increasing debris flow volumes this is the result of the conservation of mass, whereas for the increasing gravel fraction the lower velocities caused by a coarser grained front can explain higher depths. When varying solid fraction, maximum flow depth is largest at a solid content of 0.6, which is not coupled to a decrease in velocity. At the clay fraction producing the largest maximum flow velocity (Figure 5b), the lowest maximum flow depth is recorded (Figure 5f). For all variables tested, the trends in maximum discharge of the flow fronts resemble those of maximum flow depth (Figure 5i–l) due to the dependence of discharge on flow depth (see Equation 1).

Frontal flow momentum of the debris flows is similar under different gravel and solid fractions (Figure 5m,o), but increases steeply with flow volume (Figure 5p) due to its dependence on flow mass (see Equation 2). When clay fraction is varied, momentum is largest at a volumetric clay content between 0.075 and 0.1 (Figure 5n), caused by the optimum in maximum flow velocity around the same clay fraction (Figure 5b and Equation 2). The trends in calculated frontal shear stress self-evidently follow the trends in maximum flow depth (Figure 5q–t) (see Equation 1).

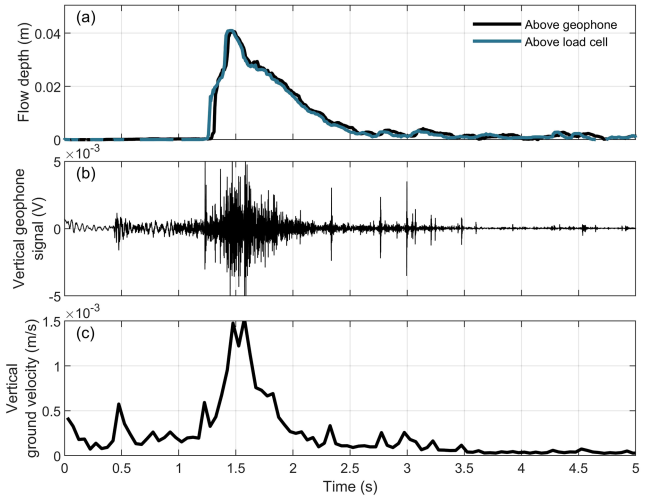

FIGURE 3 Example of output data from the flume from one of the reference experiments (experiment number 20; see Supporting Information Table 1). (a) Flow depth (m) recorded above the geophone and above the load cell; (b) vertical component of the geophone signal (V); and (c) calculated vertical ground velocity [Color figure can be viewed at wileyonlinelibrary.com]

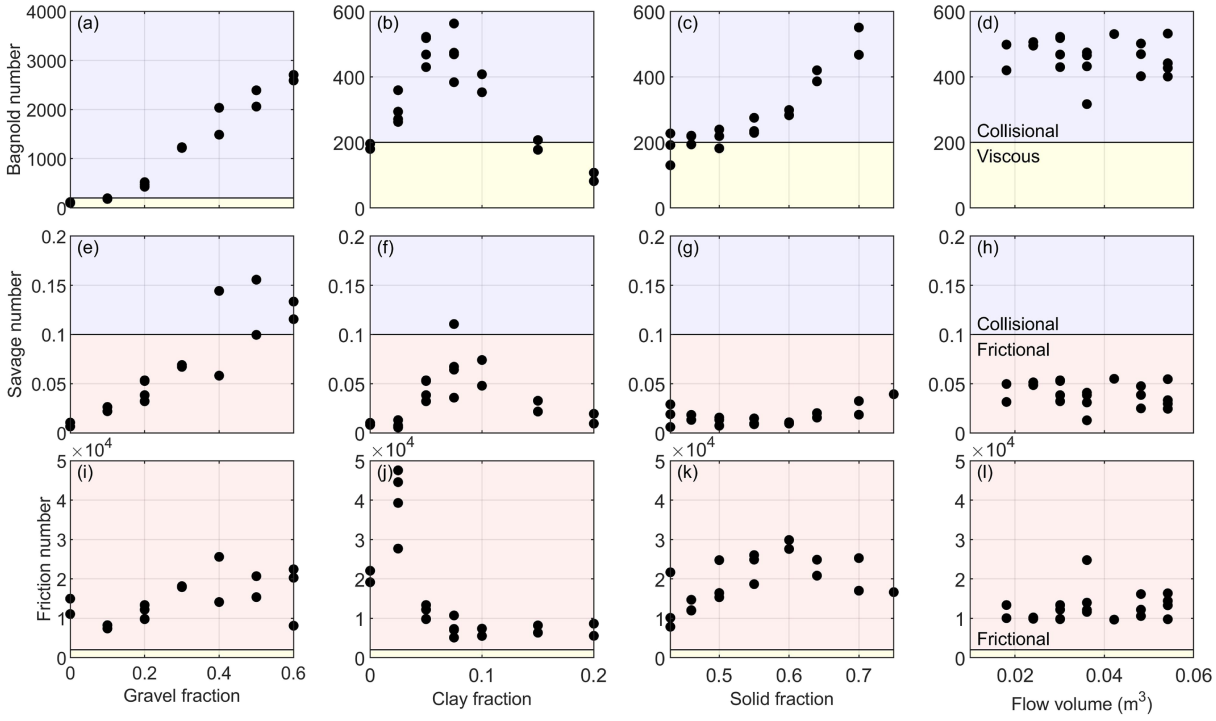

FIGURE 4 Bagnold (a–d), Savage (e–h) and friction (i–l) numbers for the four different parameters: gravel fraction, clay fraction, solid fraction and debris flow volume. Gravel and clay fractions are given as a volume fraction of the total solid volume, and solid content is given as a volume fraction of the total debris-flow volume. The horizontal lines indicate the transition from one flow regime to another. In the lowest row the black line indicates the transition from frictional to viscous forces set by Iverson (1997) [Color figure can be viewed at wileyonlinelibrary.com]

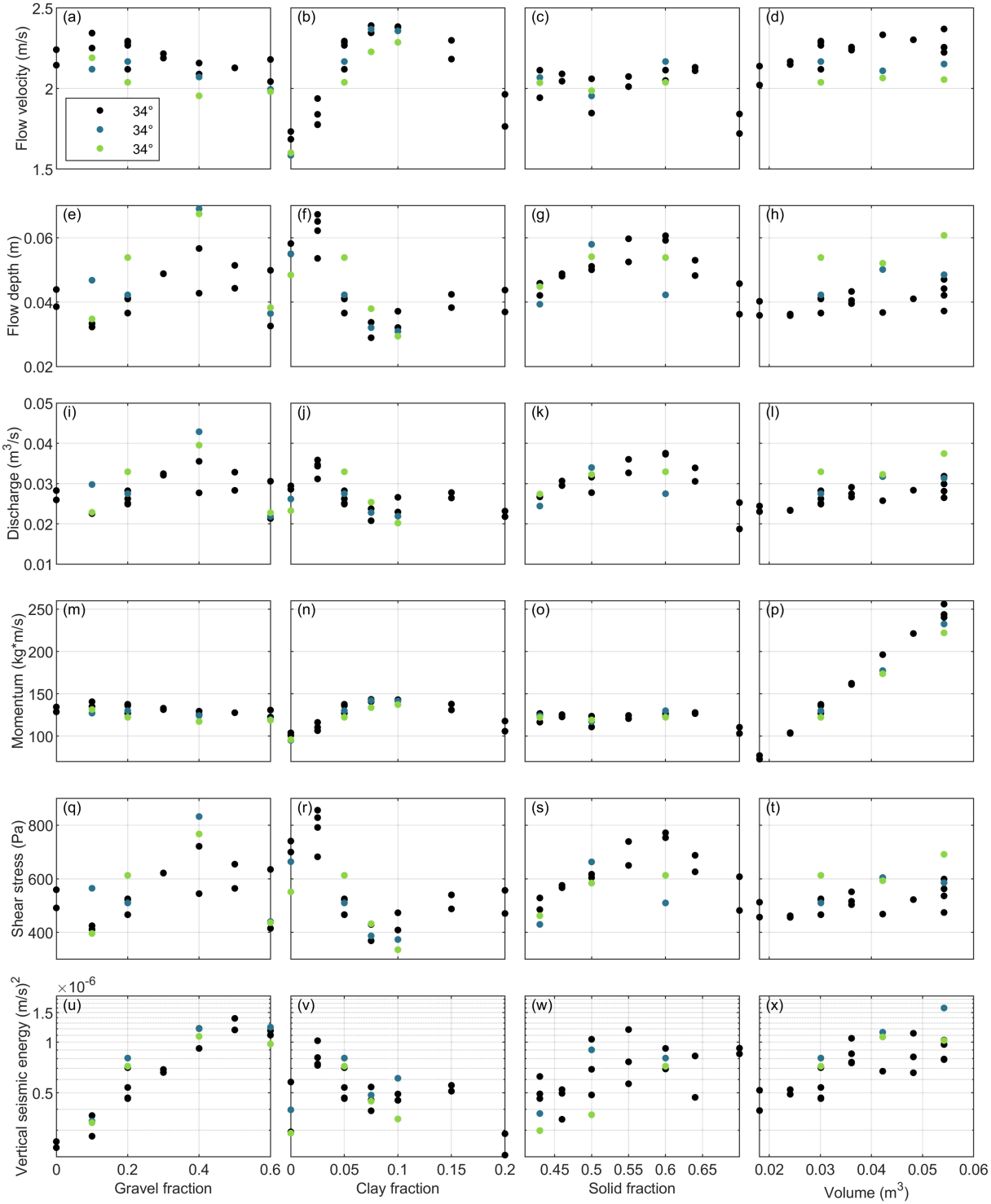

FIGURE 5 Frontal flow velocity (a–d), maximum flow depth (e–h), peak discharge (i–l), momentum (m–p), maximum shear stress (q–t) and vertical seismic energy (u–x) for the four different parameters: gravel fraction, clay fraction, solid fraction and debris flow volume. Gravel and clay fractions are given as a volume fraction of the total solid volume, and solid content is given as a fraction of the total debris-flow volume. Note that the scale of the *y*-axis of the subplots depicting vertical seismic energy (q–t) is logarithmic [Color figure can be viewed at wileyonlinelibrary.com]

The trends in the seismic energy of the debris flows very roughly resemble the trends in calculated shear stress and flow depth (Figure 5u–x—note the logarithm scale on the *y*-axes). An increase in gravel fraction results in larger seismic energies, as does an increase in flow volume. Increasing the solid volume fraction from 0.4 to 0.55 results in an increase in seismic energy. If the solid fraction increases further, seismic energy slightly decreases. When the volumetric clay fraction is varied, the smallest seismic energies are recorded at a fraction of 0 and 0.2. Under the high volumetric clay content of 0.2 the debris flow was so viscous that it stopped moving halfway in the flume, which explains the small seismic energy. Another low in seismic energy is observed around a volumetric clay content of 0.075–0.1, which coincides with the lowest maximum flow depth (see Figure 5f,v).

3.3 | General erosion patterns

The spatial patterns of erosion in the flume for the different compositions and volumes of debris flows are similar (Figure 6). Erosion is most severe at the upstream part of the erodible bed and net deposition occurs on top of the erodible bed in the downstream half of the flume. In most experiments, erosion occurs as progressive scour, and three channels are carved into the erodible bed in the upstream part. Deposition of sediment occurs in multiple lobes downstream. In the runs with large clay fractions net erosion is negligible and deposition is more uniform along the length of the flume (Figure 6c).

Despite the similarity in spatial erosion and deposition patterns in the different experiments the net change differs (Figure 7). Under increasing gravel fraction and flow volume erosion increases, whereas increasing the total solid fraction decreases erosion. These

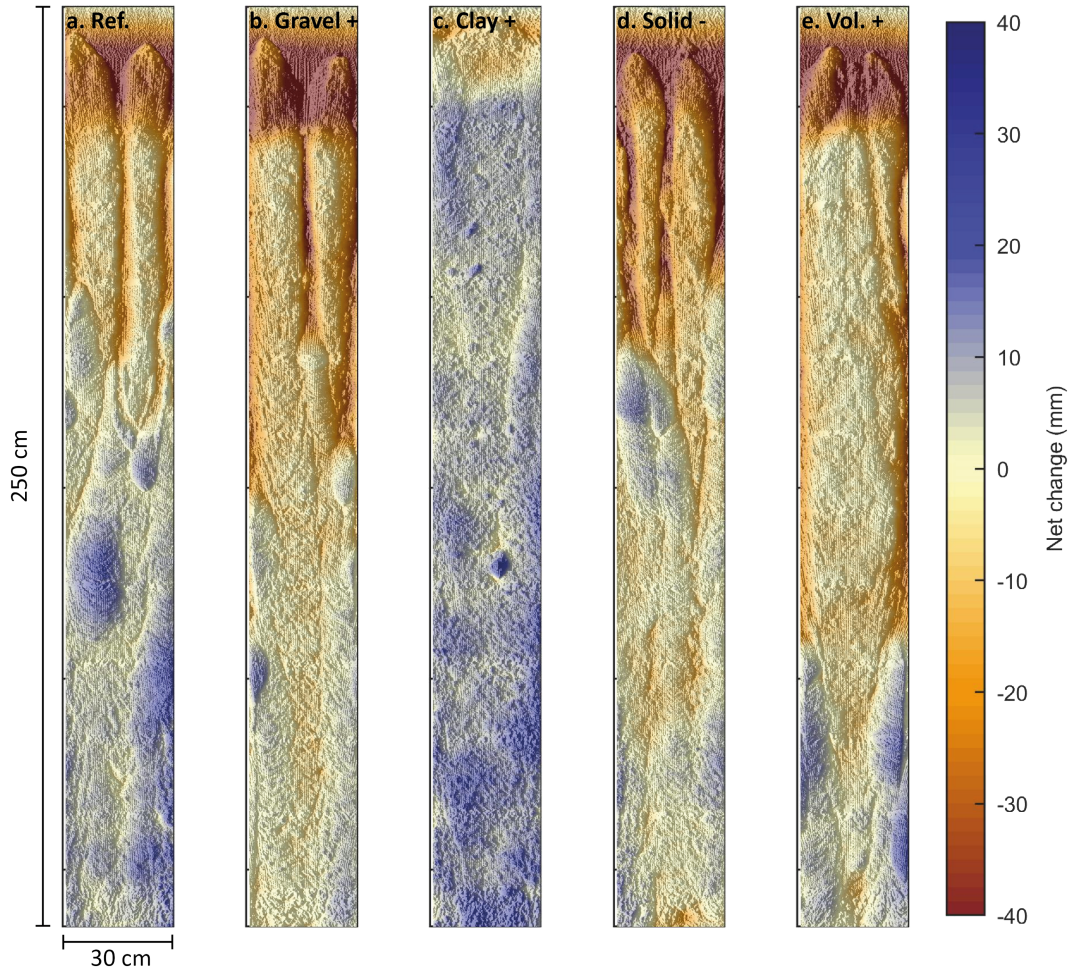

FIGURE 6 Key examples of erosion and deposition patterns in the flume. The panels shown depict the part of the flume containing the erodible bed. Panel (a) shows the pattern from one of the reference experiments (no. 6); (b) displays the results of an experiment with extra gravel (no. 28); (c) with extra clay (no. 39); (d) with a larger water-to-solid ratio (no. 56); and (e) an experiment with a larger volume (no. 12) [Color figure can be viewed at wileyonlinelibrary.com]

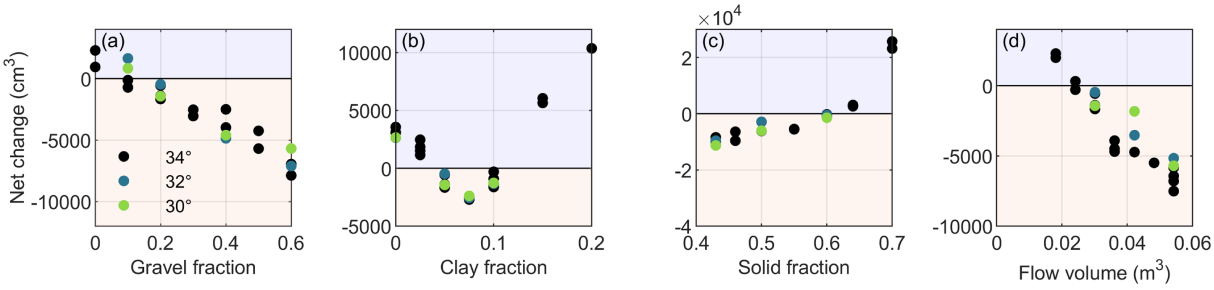

FIGURE 7 Net change above the erodible bed (cm^3) for the four different parameters tested: gravel fraction (a), clay fraction (b), solid fraction (c) and debris flow volume (d). Gravel and clay fractions are given as a volume fraction of the total solid volume, and solid content is given as a fraction of the total debris-flow volume. Note that a negative net change implies net erosion and a positive net change implies net deposition [Color figure can be viewed at wileyonlinelibrary.com]

trends can be described by simple linear relationships and are statistically significant. When the fraction of clay is varied the net change patterns become more complex. With the volumetric clay fraction increasing from 0 to 0.075 erosion increases, but when increasing the fraction of clay further from 0.1 to 0.2 erosion diminishes.

3.4 | Relation between flow characteristics and erosion

To unravel the processes and mechanisms dominating erosion, we explore the correlation between the flow characteristics of the debris flow before the erodible bed and erosion in relation to debris-flow

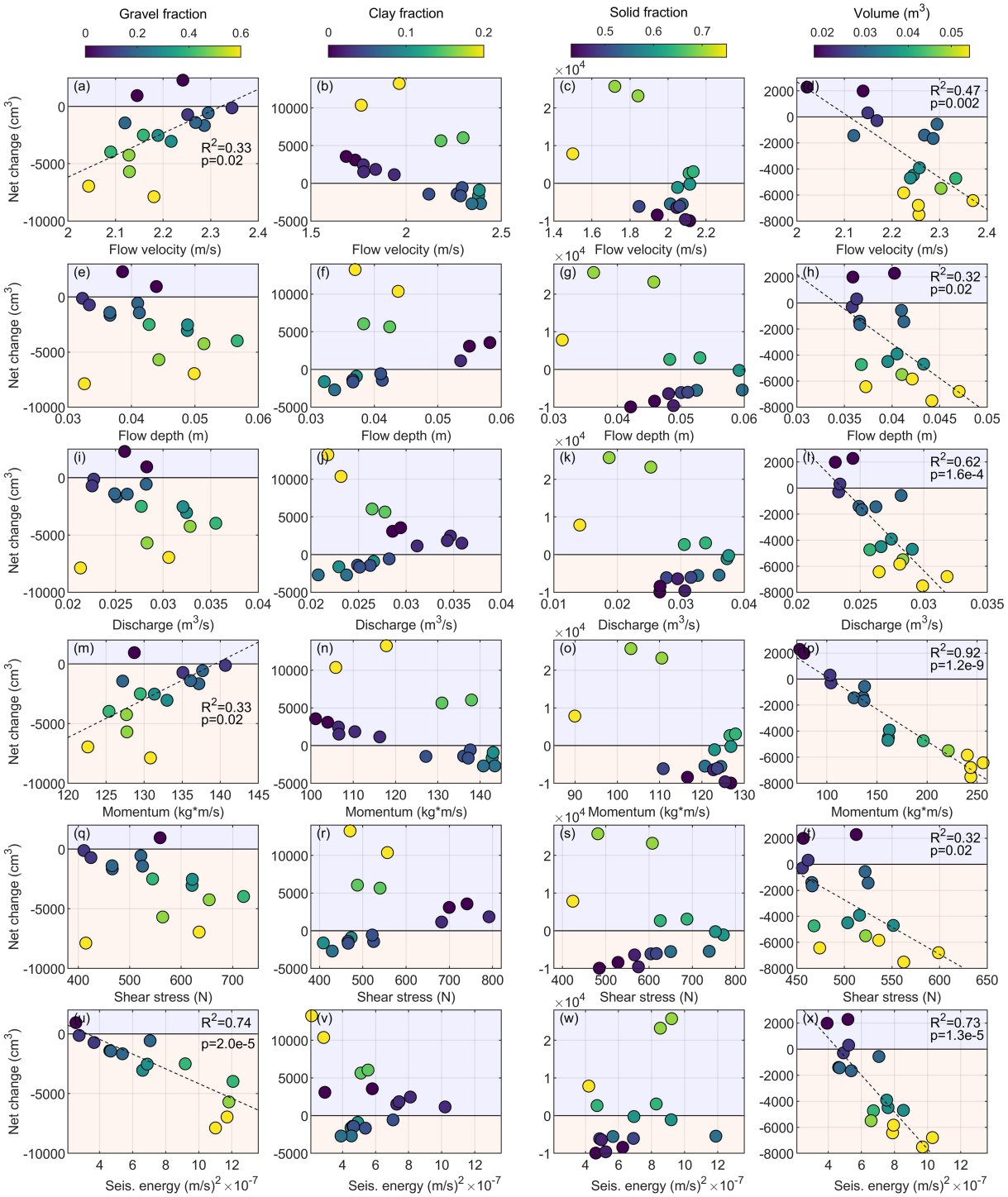

FIGURE 8 Net change above the erodible bed (cm^3), for the experiments performed at 34°, plotted as a function of frontal flow velocity (a–d), maximum flow depth (e–h), peak discharge (i–l), maximum shear stress (m–o) and vertical seismic energy (q–t) for the four different parameters tested; gravel fraction, clay fraction, solid fraction and debris flow volume, indicated with different colours. Gravel and clay fractions are given as a volume fraction of the total solid volume, and solid content is given as a fraction of the total debris-flow volume. Statistical significant linear relations are given where applicable as dotted lines, accompanied by their R^2 value. Note that a negative net change implies net erosion and a positive net change implies net deposition [Color figure can be viewed at wileyonlinelibrary.com]

composition and volume (see Figure 8). In the set of experiments in which gravel and solid fraction were varied, increased erosion generally correlated linearly to lower pre-bed frontal flow velocity and flow momentum (Figure 8a,c,m,o), except for the experiments with the highest solid fraction. For the set of experiments with increasing gravel content this trend can be explained by an increase in gravel particles at the front of the flow, slowing down the flow, while at the same time increasing impact stresses and thus erosion (Figure 8u). Hence the correlation between lower flow velocities and increased erosion does not depict causation but is merely a consequence of multiple processes influencing debris-flow mobility and erosion at the same time. For the set of experiments with increasing solid fraction the explanation behind the trend can be found in transport capacity. Increasing solid content increases the mass of the debris flow, thus increasing velocity. However, at the same time the transport capacity of the debris flow is decreased, limiting erosion. With increasing clay content or volume, an increase in frontal flow velocity and thus flow momentum linearly correlates with larger amounts of erosion, with exception of the experiments with very high clay fractions (Figure 8b,d,n,p), which follows from the basic physics describing entrainment.

When studying the relation of maximum flow depth, peak discharge and maximum shear stress before the erodible bed with net change, for varying gravel content, large scatter in the data is observed and no statistically significant linear correlation exists (Figure 8e,i,q). The relation of the data cloud to the gravel fraction itself, however, hints at a relation with a physical base that has to be studied further. An increase in maximum flow depth, and thus peak discharge and maximum shear stress, correlates significantly with an increase in erosion when volume is increased (Figure 8h,l,t). When clay fraction is increased or solid fraction is decreased, smaller maximum flow depths, peak discharges and maximum shear stresses are observed that correlate with larger amounts of erosion, with the exception of the experiments with very high clay and solid fractions (Figure 8f–g,j–k,r–s). Due to the divergent nature of the experiments with very high clay (>0.1 volume fraction) and solid fractions (>0.6 volume fraction), a simple linear relationship cannot describe the data significantly.

Under varying gravel fractions and flow volumes there is a strong and significant positive linear relation between seismic energy and net change (Figure 8u,x). However, no simple linear relation can be found between seismic energy and net change when clay and solid fractions are varied (Figure 8v,w).

3.5 | Correlation of shear and impact forces

In all sets of experiments a significant linear relation exists between vertical seismic energy and maximum shear stress (Figure 9). An increase in maximum shear stress correlates linearly with an increase in vertical seismic energy. This trend corresponds to an increase in net erosion when gravel content and volume are varied. The correlation between vertical seismic energy and maximum shear stress does not correspond to an increase in erosion when clay or solid fractions are varied.

To relate the shear and impact forces of our debris flows to their internal dynamics, we plotted them against their Bagnold and Savage numbers, respectively (Figure 10). While gravel fraction increases, increasing Bagnold numbers clearly correlate with increasing seismic energy. A similar but less clear trend can be observed in the solid fraction set, where increasing Bagnold numbers correlate with an increase in seismic energy while solid fraction increases. The trend in the solid fraction dataset between Bagnold number and the seismic energy is more scattered; however, the correlation of the scatter to the solid fraction itself points at the possibility of a relation grounded in physical processes. Increasing Bagnold numbers also result in larger seismic energy in the clay fraction set, but the scatter is large and the relation to the clay fraction itself is less clear. For the set of experiments in which volume is varied, no observable relation exists between the Bagnold number and the seismic energy.

Maximum shear stress clearly decreases when Savage numbers increase for the experiments with varying clay and solid fractions and volumes (Figure 10f–h). There is, however, no clear relation between these trends and the debris-flow composition and volume. Under varying gravel content there is no relation between the Savage number and the calculated shear stress (Figure 10e).

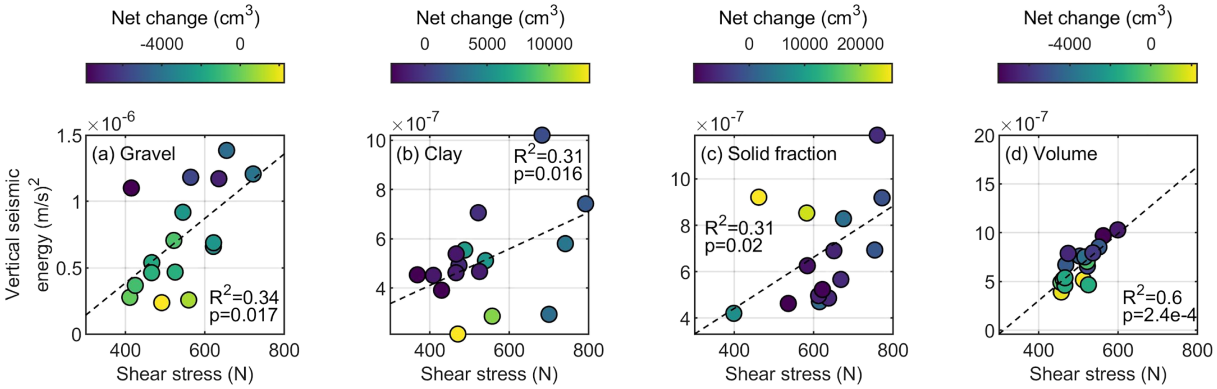

FIGURE 9 Calculated maximum shear stress (Equation 1) plotted against the measured seismic energy for the four different parameters tested: gravel fraction (a), clay fraction (b), solid fraction (c) and debris flow volume (d). Gravel and clay fractions are given as a volume fraction of the total solid volume, and solid content is given as a fraction of the total debris-flow volume. The magnitude of the net change of the individual experiments is indicated by colour. Statistically significant linear relations are given where applicable as dotted lines, accompanied by their R^2 and *p*-values [Color figure can be viewed at wileyonlinelibrary.com]

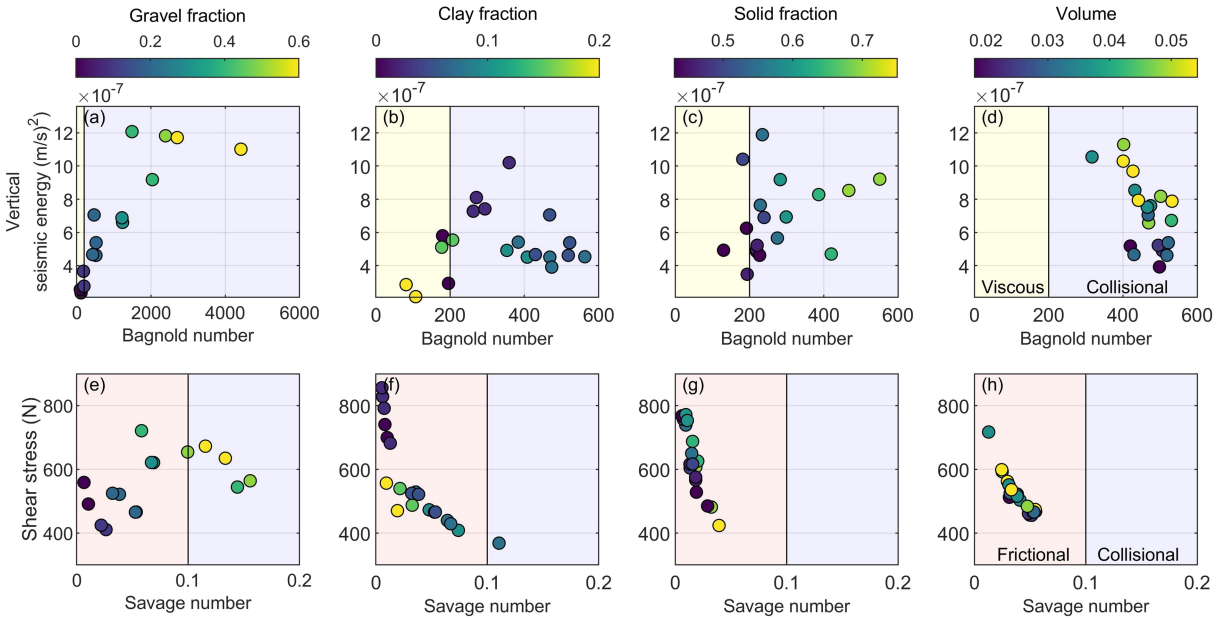

FIGURE 10 Bagnold number plotted against vertical seismic energy, a proxy for impact forces (a–d), and Savage number plotted against the calculated maximum shear stress (e–h), for the four different parameters tested; gravel fraction, clay fraction, solid fraction and debris flow volume. Gravel and clay fractions are given as a volume fraction of the total solid volume and solid content is given as a fraction of the total debris flow volume. The fraction of the gravel, clay and solid as well as the volume of the flow in m^3 are indicated by colour. The vertical lines indicate the transition from one to another flow regime [Color figure can be viewed at wileyonlinelibrary.com]

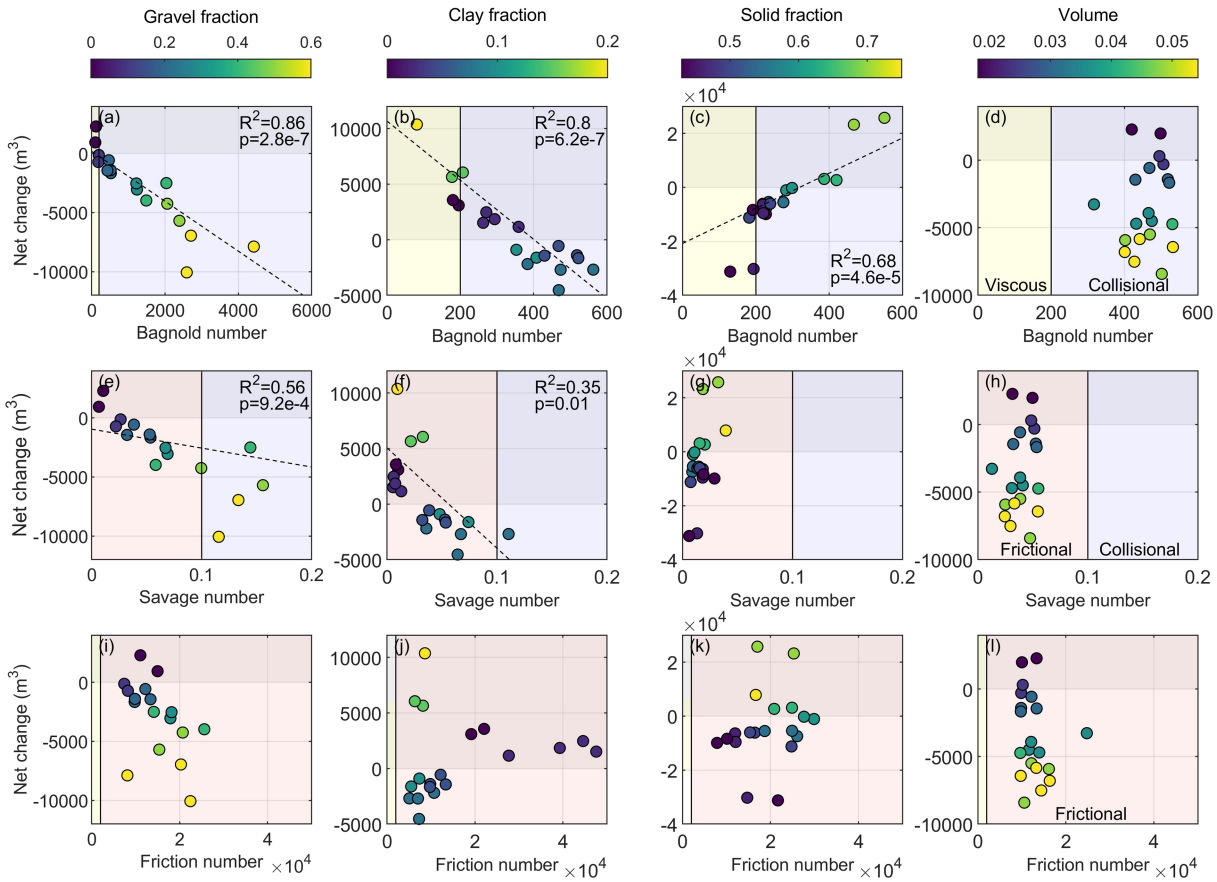

FIGURE 11 Bagnold (a–d), Savage (e–h) and friction number (i–l) plotted against net change for the four different parameters tested: gravel fraction, clay fraction, solid fraction and debris-flow volume. Gravel and clay fractions are given as a volume fraction of the total solid volume, and solid content is given as a fraction of the total debris-flow volume. The fraction of the gravel, clay and solid as well as the volume of the flow in m^3 are indicated by colour. Statistically significant linear relations are given where applicable as dotted lines, accompanied by their R^2 value. The vertical lines indicate the transition from one to another flow regime. For the friction number, the black line indicates the transition from frictional to viscous forces set by Iverson (1997) [Color figure can be viewed at wileyonlinelibrary.com]

3.6 | Dimensionless flow characterization and erosion

To characterize the possible erosional processes of the debris flows in relation to their internal dynamics further, we studied the correlation between the dimensionless Bagnold, Savage and friction numbers, and net bed change for the four different sets of experiments. Overall, we find that debris flows with low Bagnold numbers (<200), and thus a viscous flow regime, net deposition occurred (Figure 11a–d). The only exception is the flows with a low solid fraction (<0.5 volume fraction) and thus a very high water content (Figure 11c). Under varying gravel and clay fractions an increase in Bagnold number correlates linearly with an increase in erosion (Figure 11a,b). Conversely, an increase in the total solid fraction results in higher Bagnold numbers and this correlates linearly with a decrease in erosion and even deposition (Figure 11c). When only flow volume is changed, no relation is observed between Bagnold and net change (Figure 11d). The latter is as expected from the non-dimensional nature of the Bagnold number and the fact that the composition of the debris flow did not change when volume changed.

For the experiments in which gravel and clay fractions are varied, a higher Savage number corresponds to more net erosion, with the largest amount under the influence of debris flows in the collisional regime (Savage > 0.1) (Figure 11e,f). This trend positively correlates with grain size. A larger fraction of gravel corresponds to larger Savage numbers and more erosion, whereas a larger fraction of clay corresponds to smaller Savage numbers and less erosion or even deposition. In the sets of experiments where solid fraction and volume are varied, no relation exists between the Savage number and net change (Figure 11g,h). No significant relation exists between the friction number and the net change observed in our experiments (Figure 11i–l).

4 | DISCUSSION

4.1 | Effects of debris-flow composition and volume on erosion

Our experimental flows clearly show that debris-flow volume and composition influence erosion magnitude (Figure 7). The increase in erosion with debris flow volume shows that our experiments comply with earlier experimental work (Chen & Zhang, 2015; Zheng et al., 2021) and observations from the field (Schürch et al., 2011). Both in these earlier experiments and in field studies, an increase in debris flow volume correlated with an increase in flow depth, which itself correlated with the magnitude of erosion (Schürch et al., 2011; Zheng et al., 2021). In our experiments, an increase in flow volume also resulted, next to an increase in flow depth, in an increase in frontal flow velocity, frontal discharge, momentum, shear stress and seismic energy, all correlating with the increase in erosion (Figure 8d,h,l,p,t). This endorses the physical and semi-empirical formulations used in many models to describe debris flow erosion (e.g., Chen & Zhang, 2015; Dietrich & Krautblatter, 2019; Frank et al., 2015; Iverson, 2012).

In addition, the experiments with varying debris flow composition prove that the gravel, clay and total solid content have a significant effect on erosion magnitude. The tested ranges of gravel, clay and solid fraction are slightly larger than observed in nature (Yong et al., 2013), but highlight important trends, mechanisms and tipping points that should be taken into consideration when studying debris flow erosion, bulking and entrainment. Increasing the gravel content results in more erosion (Figure 7a) (as in De Haas & Woerkom, 2016; Egashira et al., 2001). Increasing the total solid content decreases erosion (Figure 7c), in agreement with Egashira et al. (2001), Hungr et al. (2005) and Fagents and Baloga (2006). This finding also corroborates the finding of Egashira et al. (2001), who proposed the existence of an upper sediment concentration limit for debris flows in motion, and the use of equilibrium volumetric solid concentrations in many numerical entrainment models (e.g., Armanini et al., 2009; Chen & Zhang, 2015), preventing models from predicting indefinite erosion. Increasing clay content has a nonlinear effect on erosion (Figure 7b), in contrast to De Haas and Woerkom (2016), who only observed a decrease in erosion due to higher clay fractions. It must, however, be noted that despite De Haas and Woerkom (2016) testing a similar range in volumetric clay fractions as we did, from 1% to 23%, they only tested four clay fractions (1%, 2%, 11% and 23%) of the total volume, whereas we tested more continuously throughout the given range.

In the experiments with varying clay fractions, only flow velocity and momentum positively correlated with erosion (Figure 8b,n). Under increasing clay fraction (from 0 to 0.1 in volume fraction), smaller flow depths, discharges and shear stresses correlated with more erosion. When gravel fraction was varied, a decrease in velocity was correlated with an increase in erosion (Figure 8a). This correlation, however, does not imply causation. An increase in gravel content increases impact forces on the bed, which increases erosion, while the slowing down of the debris flow is a secondary effect of the increased gravel content. The observation that erosion does not always correlate with flow depth, or flow velocity, under varying debris flow compositions (Figure 8a–h) hints at different mechanisms dominating erosion under debris flows with different compositions.

4.2 | Effects of debris-flow composition and volume on erosional processes: Impact and shear forces

As discussed in the Introduction, two processes are known to cause erosion under debris flows: impact and shear forces. Our experiments show that for certain experimental settings impact and shear forces correlate positively with erosion magnitude. The results from our experiments further show that the premise 'shear or impact' is incorrect. In all of our experimental sets, higher seismic energies correlated with higher shear stresses (Figure 9).

In our experimental debris flows, seismic energy—a proxy for impact forces—increases with grain size, and thus gravel fraction (Figure 5u), which is also observed by Hsu et al. (2008, 2014), He et al. (2016), Farin et al. (2019) and De Haas et al. (2021). In these specific experiments an increase in impact forces correlates with more erosion (Figure 8u). This trend is in agreement with observations on bedrock erosion by debris flows (Hsu et al., 2008, 2014; Stock & Dietrich, 2006). Our data also indicate that impact forces not only increase with increasing grain size but also with increasing debris-flow volume (Figure 5x) (as earlier concluded by De Haas et al. (2021) and

Schimmel et al. (2021), and implied in the assumptions made by Coviello et al. (2019)). The different experiments show that a doubling of gravel content and a doubling of flow volume have the same effect on the seismic response and on the eroded volume (Figures 5u,x and 8u,x). These findings suggest that when the fraction of coarse particles is high and collisional forces dominate, seismic response and possibly erosion are dominated by the collisions of gravel particles in the flow that are brought to the flow front (in correspondence with the field data of Berger et al.2011). In contrast, in our debris flow with a higher water content (volumetric solid fraction <0.5), seismic energy is lower and internal dynamics are dominated by viscous over collisional forces (according to Bagnold numbers, Figure 11c). However, erosion is still increasing (Figure 7c); an observation in line with Hungr et al. (2005), who stated that entrainment will increase with lower solid concentration. This leads to the hypothesis that under these relatively watery flows erosion does not predominantly occur underneath the debris flow front and processes other than impacts dominate erosion, such as high pore pressures, liquefaction and transport capacity of the debris flow itself.

An increase in shear stress in our experiments correlates linearly with erosion when volume is varied (Figure 8t) (in agreement with the experiments of De Haas and Woerkom, 2016, and with the physics used in the models of, e.g., Chen and Zhang, 2015, Dietrich and Krautblatter, 2019, Frank et al., 2015, and Iverson, 2012). As we calculate shear stress based on flow depth (Equation 1), this finding also corresponds to the field study of Schürch et al. (2011), who found that maximum flow depth controlled the pattern and magnitude of erosion. However, our data from the experiments with varying clay and solid fractions show that shear stress is not able to explain erosion volumes for all our experiments (Figure 8r,s). When clay or solid fractions are varied, shear stress does not correlate linearly with erosion. Shear stress is defined as the force acting by the solid boundary on the debris flow, whereas momentum is defined from the point of the moving object and momentum transfer is needed for erosion. When studying shear stress and momentum together, the relation with erosion becomes clearer. In the case of very low (volume fraction < 0.05) or very high (volume fraction > 0.1) clay contents, shear stress is high due to large flow depths but momentum of the flow and its mobility are very low, inhibiting transfer of momentum to the bed, which decreases erosion and promotes deposition. Erosion is further inhibited in flows with very high clay content, as high viscosity of the interstitial fluid inhibits the quick transfer of pore pressures from the debris flow to the bed, hindering liquefaction. In our experiments, a certain amount of flow momentum seems to be needed to overcome the shear strength of the bed, which in our experiments is equal to a momentum > 110–120 (kg m/s) (Figure 8m–p). This highlights the importance of correctly implementing momentum conservation and momentum transfer to the bed in debris flow erosion models (as earlier discussed by Iverson & Ouyang, 2015).

4.3 | Influence of the abundance and viscosity of the interstitial fluid on debris-flow dynamics and erosion

Our data show that impact and shear forces are not always able to predict erosion directly. In the experiments where clay and solid fractions are varied, impact and shear forces do not linearly correlate with erosion magnitude. As hypothesized in the Introduction, the viscosity and abundance of the interstitial fluid play a critical role in enabling and amplifying the work of erosional forces (e.g., Bagnold, 1954; Iverson, 1997; Vallance & Savage, 2000).

Our experiments show that in the absence of clay the recorded impact forces are small, and flow velocity and momentum are low (Figure 5b,n,v). This results in net deposition in the flume (Figure 7b), despite a high shear stress due to large flow depths (Figure 5f,r). In the absence of clay the transfer of water and pore pressure from debris flow to the bed happens unhindered, draining the flow and decreasing its capacity to incorporate more sediment. When clay is more abundant (volume fraction 0.05–0.1), the volume and viscosity of interstitial fluid increase, the pore pressures in our debris flows likely increase (as they also did in the experiments of Kaitna et al., 2016), while the transfer of interstitial fluid from debris flow to the bed becomes less unhindered. This allows the debris flow to keep its momentum and transport capacity, while still liquefying the bed. Under these conditions, the slight increase in clay decreases the angle of internal friction within the debris flow (Hsu et al., 2008), resulting in more mobility (also found by McArdell et al., 2007), higher flow velocities and momentum (Figure 5b,n) and slightly larger impact forces (Figure 5v) (as earlier suggested by Hsu et al., 2014). Together, this enables more erosion, despite lower shear stresses. At volumetric clay contents above 0.1 the viscosity of the interstitial fluid is so high that it starts to dominate debris-flow mobility. The high viscosity inhibits the quick transfer of interstitial fluid from the flow to the bed, and dampens the movement of the entire debris flow as well as the movement of individual sediment particles, preventing the formation of a large coarse front and decreasing impact forces on the bed (as earlier concluded by, among others, Iverson, 1997; Major & Iverson, 1999; McCoy et al., 2010). Under these clay-rich conditions, despite slightly higher shear stresses, erosion completely diminishes (Figure 7b). Our experiments with varying clay contents seem to comply with contrasting conclusions on the effects of viscosity on debris-flow dynamics from different studies. On the one hand, studies conclude that impact forces decrease when the viscosity of the interstitial fluid increases (e.g., Iverson, 1997; Major & Iverson, 1999; McCoy et al., 2010), whereas others say that impact forces increase with higher clay content (Hsu et al., 2014). We therefore hypothesize that previous studies captured only one half of the nonlinear effect of clay content and interstitial viscosity. Our broad range of tested clay fractions unifies these previously contrasting observations.

The experiments with varying solid content further underline the importance of the abundance of interstitial fluid. When volumetric solid content is increased from 0.4 to 0.6, flow depth, shear stress and seismic energy increase, but erosion decreases (Figures 5g,s,w and 7c). For a further increase in solid content, up to 0.7, flow depth, shear stress and impact forces become smaller, further decreasing erosion and enhancing deposition. If we follow the line of reasoning on transport capacity by Takahashi (1981) and Hungr et al. (2005), we can assume that at these high solid fractions the debris flows are becoming saturated by solids and are not able to incorporate more loose material. In addition, high pore pressures, and thus a larger water content, can aid entrainment by reducing grain-to-grain basal friction (e.g., Iverson et al.2011; Li et al., 2020) and increasing liquefaction (e.g., Hungr et al., 2005; Sassa & hui Wang, 2005).

Our experimental findings on the effects of solid content of the debris flow on erosion are consistent with the hypothesis of Iverson et al. (2011) and Iverson (2012). They stated that a high bed wetness, resulting in high and contrasting pore pressures between the bed and debris flow, is important for promoting entrainment. Their experimental results showed that high pore pressures generated as wet bed sediment are overridden and entrained can result in liquefaction (Iverson, 2012), causing a reduction in grain-to-grain friction, an increase in flow momentum and further erosion (Iverson et al., 2011). Our results add to their findings by showing that not only bed wetness influences erosion, but water content and the viscosity of the interstitial fluid of the debris flow itself affect erosion and erosional processes of loose sediment, by changing pore pressures and momentum of the flow, influencing the transfer of interstitial fluid from flow to bed and changing the transport capacity of the flow itself. The similarity in observations between Iverson et al. (2011), Iverson (2012) and this study on the effects of water content raises questions on how clay content of the bed affects erosion and whether those effects will be similar to the effects of clay content of the debris flow on erosion.

4.4 | Internal debris flow dynamics in relation to erosion

The experiments provide evidence that the internal dynamics of debris flows correspond to the forces, impact and shear, working on the bed underneath a debris flow (Figures 10 and 11). With varying gravel content and solid fractions an increase in the seismic signal correlated with higher Bagnold numbers—that is, collisional regime (Figure 10a,c). With varying clay fractions, solid fractions and volumes, larger shear stresses correlated with lower Savage numbers—that is, frictional regime (Figure 10f–h).

The trends in the Bagnold and Savage numbers, for the experiments in which gravel and clay were varied, also correlate linearly with net change (Figure 11a,b,e,f). This provides evidence that the internal debris-flow dynamics not only correspond to the forces working on the bed but also the actual erosion. More collisional behaviour in the debris flows—that is, higher Bagnold numbers and higher Savage numbers—corresponded to more erosion (Figure 11a,b,e,f). When gravel fraction is increased this is directly linked to the observed increase in seismic energy, and thus impacts on the bed. The linear relation between erosion and Bagnold and Savage numbers for the experiments with varying clay content is, however, more surprising, as the erosion magnitude under varying clay content is nonlinear. The erosive behaviour of debris flows with varying clay contents is the result of a multitude of different physical mechanisms working on the bed (e.g., impact and shear forces, viscosity of the interstitial fluid, pore pressure transfer, momentum) that are captured by these non-dimensional numbers.

The only erosion-influencing factor that is not captured well by the non-dimensional numbers used in this paper (Bagnold, Savage and friction) is the transport capacity of the flow. When solid fraction is varied, no positive linear relation exists between erosion and these non-dimensional numbers (Figure 11c,g,k). The negative relation between erosion and the Bagnold number when solid content is varied (Figure 11c) is a direct result of the increase in solid content v_s. The increase in predicted collisional behaviour is, however, baffled by the lack of transport capacity of the flow and the limited transfer of water and pore pressure from the flow to the bed in these sediment-saturated flows.

4.5 | Implications on the prediction and modelling of debris flow erosion and entrainment in the field

Our experimental data show that when debris-flow composition is relatively stable both seismic signals and shear stresses can be used to predict debris-flow erosion, entrainment and volume growth in the field, and that we could use both forces in modelling debris-flow erosion (Figure 8t,x). Our data, however, also show that we should be careful with direct and simplified predictions based on solely shear stress or impact forces if debris-flow composition varies greatly between debris-flow sites, events or even within events (Figure 8r,s,v,w).

When the abundance or viscosity of the interstitial fluid of a debris flow differs, the internal dynamics of the debris flow and erosion are significantly affected (Figures 7b and 11b,f). This is in line with earlier statements and conclusions on the importance and means of momentum exchange for models and our understanding of erosional processes (e.g., Dietrich & Krautblatter, 2019; Iverson & Ouyang, 2015; Li et al., 2020; Ouyang et al., 2015). Li et al. (2020) explained that different types of dominant stresses within debris-flow mixtures correspond to different momentum transport processes that govern and influence erosion. The effects of the abundance or viscosity of the interstitial fluid on the dynamics of our experimental debris flow are complex and not linear with either shear stress or impact forces (Figure 5r,s,v,w). However, according to our data, water content does have a positive linear effect on debris-flow erosion (Figure 7c), which is likely coupled to pore pressures, liquefaction and transport capacity.

Our data also shed light on the discussion under which part of the debris flow most erosion occurs—the flow front or the tail. Despite measuring erosion only after the passage of an entire debris flow in our flume, the wide variety of tested debris flow compositions leaves room for interpretation and discussion. As discussed earlier, the experiments with varying gravel fractions and volumes show that impact forces are largest underneath the debris-flow front, and that seismic energy in these experimental sets correlates strongly with erosion (Figure 8u,x). An increase in gravel particles causes thicker and coarser-grained flow fronts in our experiments due to particle segregation, which enhances impact forces and thus erosion. Our experiments, therefore, enforce earlier hypotheses by Berger et al. (2011) and Stock and Dietrich (2006) stating that most erosion happens underneath the flow front. In contrast, the data from our experiments with a high water content show that even with smaller impact forces large amounts of erosion can occur (Figure 8w), which is in line with (Hungr et al., 2005), who expected that flows with lower sediment concentrations are more erosive. We therefore hypothesize that whether erosion dominantly occurs underneath the flow front, tail or both depends on the interplay between the composition of the debris flow, the erosive forces working on the bed, the efficiency of momentum transfer to the bed and the conditions of the overridden bed. When the bed conditions are erosion prone—that is, loosely packed

wet sediment (Iverson et al., 2011), erosion will occur underneath collision-dominated flow fronts by impact forces and underneath more watery flow fronts and tails by increased pore pressure and liquefaction. Therefore, it becomes clear that debris flow erosion cannot be estimated by the sum of different factors but that the interplay of these factors determines erosion. This has great implications for the modelling of debris-flow erosion. Where the incorporation of an equilibrium sediment concentration by Armanini et al. (2009) is a step in the right direction, their current model does not consider the erosive forces of the debris flow, resulting in unrealistic magnitudes of erosion in some places (Gregoretti et al., 2019). Other models describing debris-flow erosion do incorporate the most important erosive forces, shear and impact, but do not consider the nonlinear effects of clay within the interstitial fluid and the transport capacity of the debris flows. Both these factors influence how, and how effectively, momentum is transferred from the debris flow to the bed.

To summarize our findings and therefore the implications for erosion modelling, we can state that erosion caused by debris flows (E_{DF}) is a function of impact (F_I) and shear forces (F_τ), and the means and effectiveness of pore pressure transfer between the debris flow and the bed ($P_{DF\leftrightarrow B}$):

$$E_{DF} = f(F_I, F_\tau, M_{DF\leftrightarrow B}), \tag{8}$$

in which impact forces are predominantly a function of the grain size (D), the viscosity of the interstitial fluid (μ), flow depth (H) and flow velocity (u):

$$F_I = f(D, \mu, H, u), \tag{9}$$

and shear forces are a function of the debris flow density (ρ), flow depth and slope (S), as already defined in Equation (1):

$$F_\tau = f(\rho, H, S), \tag{10}$$

in which H itself is also influenced by the composition of the debris flow and its velocity. The means and effectiveness of elevated pore pressure transfer are influenced by the viscosity of the interstitial fluid and the fraction of solids (v_s):

$$P_{DF\leftrightarrow B} = f(\mu, v_s). \tag{11}$$

As our data show, the interaction between all these parameters is complex, dependent on debris-flow composition, and often nonlinear, especially when clay fraction is varied and water content of the debris flow is limited. The complex interplay between these forces and mechanisms is, nonetheless, also key in accurately describing debris-flow erosion. We therefore recommend incorporating the nonlinear effects of the abundance and viscosity of the interstitial fluid on debris-flow dynamics, and erosional processes in erosion prediction and entrainment modelling. An opportunity for simple incorporation may lay in the linear relation between flow momentum and erosion under varying clay fractions, as the viscosity of the interstitial fluid directly influences debris-flow movement. The linear relation between solid fraction and erosion also brings the potential for simple model implementation as well as the relationships between the internal dynamics, classified by Bagnold and Savage numbers, and erosion. Changes in debris-flow composition as entrainment continues should ideally be accounted for, as well as how bed composition itself affects debris-flow erosion. The importance of the latter has been shown by Iverson et al. (2011), but has to be explored and studied further. An additional complicating factor in the field is the availability of loose sediments (Simoni et al., 2020), a factor not studied in this paper. Solving the erosion functions above is beyond the scope of this paper, as we would also need to include the effects of the conditions of the bed to fully describe erosion of loose sediment by debris flows.

5 | CONCLUSIONS

We experimentally investigated the effects of debris-flow composition and volume on debris-flow erosion and erosional mechanisms. By releasing 96 debris flows in a flume, 5.4 m long and 0.3 m wide, with an erodible bed, we tested the erosional power of different debris-flow compositions and volumes. With data of our distance sensors and geophone we were able to quantify the shear and impact forces working on the bed and infer the importance of flow momentum and the characteristics of the interstitial fluid.

Our experiments show that debris-flow erosion and erosional processes depend on debris-flow composition and volume. Erosion increases when the fraction or total volume of gravel in a debris flow is increased. Enhanced erosion as a result of debris-flow composition is established, in general, through increasing impact and shear forces on the bed. When gravel fraction or total volume is increased, the recorded impact force and shear stress increase, and therefore also the eroded volume. This implies that both erosional forces, impact and shear, are connected in natural debris flows and can be used to predict debris flow erosion in most cases.

The experiments in this study, however, also show that the influence of the abundance and viscosity of the interstitial fluid complicates the predictability of debris-flow erosion based on either shear or impact forces, by changing the means and effectiveness of pore pressure transfer between the debris flow and the bed. Debris-flow erosion, in our experiments, is enhanced by an abundance of water and is optimal around a volumetric clay fraction of 0.075 when the total solid volume fraction is 0.6. Under these conditions, flow velocities and impact forces are high and, according to literature, large differences in pore pressure between the debris flow and the bed likely exist, resulting in large momentum and effective pore pressure transfer and thus large amounts of erosion despite relatively low shear stresses. Too much clay (volume fraction > 0.075) increases the viscosity of the interstitial fluid to a degree of flow immobility, small flow momentum, low impact forces, diminishing transfer of pore pressure from the debris flow to the bed and, ultimately, no net erosion. At the same time, absence of clay also decreases flow mobility and momentum, by rapid draining of water from the debris flow to the bed. The drainage of water from debris flow to the bed decreases mobility of the flow quickly, decreases pressure differences and increases the angle of internal friction between the grains in the debris flow, resulting in little to no erosion.

We recommend incorporating the nonlinear effects of the abundance and viscosity of the interstitial fluid on debris flow dynamics and erosional processes in entrainment modelling. Changes in debris-flow composition as entrainment continues should ideally be accounted for, as well as how the bed composition itself affects

debris-flow erosion. For erosion and volume prediction in the field we advise to account for the nonlinear effects of interstitial fluid when debris-flow composition differs greatly between events, or when comparing various debris-flow sites. In these cases, data from load cells, distance sensors and pore-pressure sensors could be used to estimate interstitial fluid viscosity and abundance indirectly.

We can also conclude that the forces that dominate internal dynamics of debris flows are similar to those that dictate erosion. Thereby, dimensionless numbers used to categorize debris flows can also be used as indicators for debris-flow erosion potential and erosional mechanisms when comparing debris flows of different compositions.

ACKNOWLEDGEMENTS

This work was supported by the Netherlands Organisation for Scientific Research (NWO) (grants 0.16.Veni.192.001 and OCENW.KLEIN.495 to TdH). The authors gratefully acknowledge Arjan van Eijk, Bas van Dam, Marcel van Maarseveen, Henk Markies and Mark Eijkelboom for their help with the design and construction of the flume and measurement set-up, as well as their assistance during the experiments. The authors would also like to gratefully acknowledge the assistance of Kees van Welsum in conducting the experiments and Maarten Kleinhans in providing us with a first internal review. We would also like to thank two anonymous reviewers. Their constructive feedback greatly improved this manuscript.

AUTHOR CONTRIBUTIONS

Lonneke Roelofs conceived the study and wrote the paper. Tjalling de Haas reviewed and edited the initial draft in detail, and designed the laboratory facility. Both Tjalling de Haas and Lonneke Roelofs contributed to the conceptualization and the development of the experimental methods and data analyses. Lonneke Roelofs and Pauline Colucci executed the experiments, and collected and processed the data. All authors contributed to idea development and manuscript preparation.

Data availability statement

DEMs and raw data from the sensors in the flume are made available via Yoda (online repository of Utrecht University). The data and an instruction on how we processed the raw data can be found under this link: https://public.yoda.uu.nl/geo/UU01/7WFE5C.html. DOI: 10.24416/UU01-7WFE5C.

ORCID

Lonneke Roelofs https://orcid.org/0000-0001-6993-6470
Tjalling de Haas https://orcid.org/0000-0001-8949-3929

REFERENCES

Abancó C., Hürlimann M. (2014) Estimate of the debris-flow entrainment using field and topographical data. *Natural Hazards*, 71(1), 363–383.

Armanini A., Fraccarollo L., Rosatti G. (2009) Two-dimensional simulation of debris flows in erodible channels. *Computers & Geosciences*, 35(5), 993–1006.

Baggio T., Mergili M., D'Agostino V. (2021) Advances in the simulation of debris flow erosion: The case study of the rio gere (italy) event of the 4th august 2017. *Geomorphology*, 381, 107664.

Bagnold R.A. (1954) Experiments on a gravity-free dispersion of large solid spheres in a newtonian fluid under shear. *Proceedings of the Royal Society of London. Series A. Mathematical and Physical Sciences*, 225 (1160), 49–63.

Beaty C.B. (1963) Origin of alluvial fans, white mountains, california and nevada. *Annals of the Association of American Geographers*, 53(4), 516–535.

Berger C., McArdell B.W., Schlunegger F. (2011) Direct measurement of channel erosion by debris flows, illgraben, switzerland. *Journal of Geophysical Research: Earth Surface*, 116(F1), F01002.

Blair T.C., McPherson J.G. (1994) Alluvial fans and their natural distinction from rivers based on morphology, hydraulic processes, sedimentary processes, and facies assemblages. *Journal of sedimentary research*, 64(3a), 450–489.

Chen H.X., Zhang L.M. (2015) Edda 1.0: integrated simulation of debris flow erosion, deposition and property changes. *Geoscientific Model Development*, 8(3), 829–844.

Costa J.E. (1984) Physical geomorphology of debris flows. In *Developments and applications of geomorphology*, Springer; 268–317.

Coviello V., Arattano M., Comiti F., Macconi P., Marchi L. (2019) Seismic characterization of debris flows: insights into energy radiation and implications for warning. *Journal of Geophysical Research: Earth Surface*, 124(6), 1440–1463.

De Haas T., Åberg A.S., Walter F., Zhang Z. (2021) Deciphering seismic and normal-force fluctuation signatures of debris flows: An experimental assessment of effects of flow composition and dynamics. *Earth Surface Processes and Landforms*, 46, 2195–2210.

De Haas T., Braat L., Leuven J. asperR. F. W., Lokhorst I.R., Kleinhans M.G. (2015) Effects of debris flow composition on runout, depositional mechanisms, and deposit morphology in laboratory experiments. *Journal of Geophysical Research: Earth Surface*, 120(9), 1949–1972.

De Haas T., Nijland W., De Jong S.M., McArdell B.W. (2020) How memory effects, check dams, and channel geometry control erosion and deposition by debris flows. *Scientific reports*, 10(1), 1–8.

De Haas T., Ventra D., Carbonneau P.E., Kleinhans M.G. (2014) Debris-flow dominance of alluvial fans masked by runoff reworking and weathering. *Geomorphology*, 217, 165–181.

De Haas T., Woerkom T. (2016) Bed scour by debris flows: experimental investigation of effects of debris-flow composition. *Earth Surface Processes and Landforms*, 41(13), 1951–1966.

Dietrich A., Krautblatter M. (2019) Deciphering controls for debris-flow erosion derived from a lidar-recorded extreme event and a calibrated numerical model (roßbichelbach, germany). *Earth Surface Processes and Landforms*, 44(6), 1346–1361.

Dowling C.A., Santi P.M. (2014) Debris flows and their toll on human life: a global analysis of debris-flow fatalities from 1950 to 2011. *Natural hazards*, 71(1), 203–227.

Egashira S., Honda N., Itoh T. (2001) Experimental study on the entrainment of bed material into debris flow. *Physics and Chemistry of the Earth, Part C: Solar, Terrestrial & Planetary Science*, 26(9), 645–650.

Fagents S.A., Baloga S.M. (2006) Toward a model for the bulking and debulking of lahars. *Journal of Geophysical Research: Solid Earth*, 111 (B10), B10201.

Farin M., Tsai V.C., Lamb M.P., Allstadt K.E. (2019) A physical model of the high-frequency seismic signal generated by debris flows. *Earth Surface Processes and Landforms*, 44(13), 2529–2543.

Frank F., McArdell B.W., Huggel C., Vieli A. (2015) The importance of erosion for debris flow runout modelling from applications to the swiss alps. *Natural Hazards & Earth System Sciences Discussions*, 3(4), 2379–2417.

Frank F., McArdell B.W., Oggier N., Baer P., Christen M., Vieli A. (2017) Debris-flow modeling at meretschibach and bondasca catchments, switzerland: sensitivity testing of field-data-based entrainment model. *Natural hazards and earth system sciences*, 17 (5), 801–815.

Gregoretti C., Stancanelli L.M., Bernard M., Boreggio M., Degetto M., Lanzoni S. (2019) Relevance of erosion processes when modelling in-channel gravel debris flows for efficient hazard assessment. *Journal of Hydrology*, 568, 575–591.

Han Z., Chen G., Li Y., Zhang H., He Y. (2016) Elementary analysis on the bed-sediment entrainment by debris flow and its application using the topflowdf model. *Geomatics, Natural Hazards and Risk*, 7(2), 764–785.

He S., Liu W., Li X. (2016) Prediction of impact force of debris flows based on distribution and size of particles. *Environmental Earth Sciences*, 75 (4), 298.

Hoefling R. (2004) High-speed 3d imaging by dmd technology, Machine vision applications in industrial inspection XII; 188–194.

Hsu L., Dietrich W.E., Sklar L.S. (2008) Experimental study of bedrock erosion by granular flows. *Journal of Geophysical Research: Earth Surface*, 113(F2), F02001.

Hsu L., Dietrich W.E., Sklar L.S. (2014) Mean and fluctuating basal forces generated by granular flows: Laboratory observations in a large vertically rotating drum. *Journal of Geophysical Research: Earth Surface*, 119(6), 1283–1309.

Hungr O. (1999) Analysis of debris flow surges using the theory of uniformly progressive flow. *Earth Surface Processes and Landforms: The Journal of the British Geomorphological Research Group*, 25(5), 483–495.

Hungr O., McDougall S., Bovis M. (2005) Entrainment of material by debris flows. In *Entrainment of material by debris flows. in debris flow hazards and related phenomena*, Springer Berlin Heidelberg; 135–158.

Iverson R.M. (1997) The physics of debris flows. *Reviews of geophysics*, 35 (3), 245–296.

Iverson R.M. (2012) Elementary theory of bed-sediment entrainment by debris flows and avalanches. *Journal of Geophysical Research: Earth Surface*, 117(F3), F03006.

Iverson R.M., Denlinger R.P. (2001) Flow of variably fluidized granular masses across three-dimensional terrain: 1. coulomb mixture theory. *Journal of Geophysical Research: Solid Earth*, 106(B1), 537–552.

Iverson R.M., Logan M., LaHusen R.G., Berti M. (2010) The perfect debris flow? aggregated results from 28 large-scale experiments. *Journal of Geophysical Research: Earth Surface*, 115(F3), F03005.

Iverson R.M., Ouyang C. (2015) Entrainment of bed material by earth-surface mass flows: Review and reformulation of depth-integrated theory. *Reviews of Geophysics*, 53(1), 27–58.

Iverson R.M., Reid M.E., Logan M., LaHusen R.G., Godt J.W., Griswold J.P. (2011) Positive feedback and momentum growth during debris-flow entrainment of wet bed sediment. *Nature Geoscience*, 4(2), 116–121.

Jeong S.W. (2010) Grain size dependent rheology on the mobility of debris flows. *Geosciences Journal*, 14(4), 359–369.

Kaitna R., Palucis M.C., Yohannes B., Hill K.M., Dietrich W.E. (2016) Effects of coarse grain size distribution and fine particle content on pore fluid pressure and shear behavior in experimental debris flows. *Journal of Geophysical Research: Earth Surface*, 121(2), 415–441.

Kang C., Chan D. (2018) A progressive entrainment runout model for debris flow analysis and its application. *Geomorphology*, 323, 25–40.

Lanzoni S., Gregoretti C., Stancanelli L.M. (2017) Coarse-grained debris flow dynamics on erodible beds. *Journal of Geophysical Research: Earth Surface*, 122(3), 592–614.

Li Y., Liu J., Su F., Xie J., Wang B. (2015) Relationship between grain composition and debris flow characteristics: a case study of the jiangjia gully in china. *Landslides*, 12(1), 19–28.

Li P., Wang J., Hu K., Wang F. (2020) Experimental study of debris-flow entrainment over stepped-gradient beds incorporating bed sediment porosity. *Engineering Geology*, 274, 105708.

Liu D., Li Y., You Y., Liu J., Wang B., Yu B. (2020) Velocity of debris flow determined by grain composition. *Journal of Hydraulic Engineering*, 146(8), 06020010.

Major J.J. (2000) Gravity-driven consolidation of granular slurries: implications for debris-flow deposition and deposit characteristics. *Journal of Sedimentary Research*, 70(1), 64–83.

Major J.J., Iverson R.M. (1999) Debris-flow deposition: Effects of pore-fluid pressure and friction concentrated at flow margins. *Geological Society of America Bulletin*, 111(10), 1424–1434.

Major J.J., Pierson T.C. (1992) Debris flow rheology: Experimental analysis of fine-grained slurries. *Water resources research*, 28(3), 841–857.

Major J.J., Voight B. (1986) Sedimentology and clast orientations of the 18 may 1980 southwest-flank lahars, mount st. helens, washington. *Journal of Sedimentary Research*, 56(5), 691–705.

Mangeney A., Bouchut F., Thomas N., Vilotte J.-P., Bristeau M.O. (2007) Numerical modeling of self-channeling granular flows and of their levee-channel deposits. *Journal of Geophysical Research: Earth Surface*, 112(F2), F02017.

McArdell B.W., Bartelt P., Kowalski J. (2007) Field observations of basal forces and fluid pore pressure in a debris flow. *Geophysical research letters*, 34, L07406.

McCoy S.W., Kean J.W., Coe J.A., Staley D.M., Wasklewicz T.A., Tucker G. E. (2010) Evolution of a natural debris flow: In situ measurements of flow dynamics, video imagery, and terrestrial laser scanning. *Geology*, 38(8), 735–738.

McCoy S.W., Kean J.W., Coe J.A., Tucker G.E., Staley D.M., Wasklewicz T. A. (2012) Sediment entrainment by debris flows: In situ measurements from the headwaters of a steep catchment. *Journal of Geophysical Research: Earth Surface*, 117, F03016.

McCoy S.W., Tucker G.E., Kean J.W., Coe J.A. (2013) Field measurement of basal forces generated by erosive debris flows. *Journal of Geophysical Research: Earth Surface*, 118(2), 589–602.

McGuire L.A., Rengers F.K., Kean J.W., Staley D.M. (2017) Debris flow initiation by runoff in a recently burned basin: Is grain-by-grain sediment bulking or en masse failure to blame? *Geophysical Research Letters*, 44(14), 7310–7319.

Navratil O., Liébault F., Bellot H., Travaglini E., Theule J., Chambon G., Laigle D. (2013) High-frequency monitoring of debris-flow propagation along the réal torrent, southern french prealps. *Geomorphology*, 201, 157–171.

O'Brien J.S., Julien P.Y. (1988) Laboratory analysis of mudflow properties. *Journal of hydraulic engineering*, 114(8), 877–887.

Ouyang C., He S., Tang C. (2015) Numerical analysis of dynamics of debris flow over erodible beds in wenchuan earthquake-induced area. *Engineering Geology*, 194, 62–72.

Paola C., Straub K., Mohrig D., Reinhardt L. (2009) The "unreasonable effectiveness" of stratigraphic and geomorphic experiments. *Earth-Science Reviews*, 97(1-4), 1–43.

Parsons J.D., Whipple K.X., Simoni A. (2001) Experimental study of the grain-flow, fluid-mud transition in debris flows. *The Journal of Geology*, 109(4), 427–447.

Phillips C.J., Davies T. imothyR. H. (1991) Determining rheological parameters of debris flow material. *Geomorphology*, 4(2), 101–110.

Pierson T.C. (1986) Flow behavior of channelized debris flows, mount st. helens, washington, Hillslope processes.

Pudasaini S.P., Fischer J.-T. (2020) A mechanical erosion model for two-phase mass flows. *International Journal of Multiphase Flow*, 132, 103416.

Reid M.E., Coe J.A., Brien D.L. (2016) Forecasting inundation from debris flows that grow volumetrically during travel, with application to the oregon coast range, usa. *Geomorphology*, 273, 396–411.

Rengers F.K., McGuire L.A., Kean J.W., Staley D.M., Dobre M., Robichaud P.R., Swetnam T. (2021) Movement of sediment through a burned landscape: Sediment volume observations and model comparisons in the san gabriel mountains, california, usa. *Journal of Geophysical Research: Earth Surface*, 126(7), e2020JF006053.

Rickenmann D. (1999) Empirical relationships for debris flows. *Natural hazards*, 19(1), 47–77.

Rickenmann D. (2005) Runout prediction methods. In *Debris-flow hazards and related phenomena*, Springer Berlin Heidelberg; 305–324.

Santi P.M., deWolfe V.G., Higgins J.D., Cannon S.H., Gartner J.E. (2008) Sources of debris flow material in burned areas. *Geomorphology*, 96 (3-4), 310–321.

Sassa K., Wang G. (2005) Mechanism of landslide-triggered debris flows: Liquefaction phenomena due to the undrained loading of torrent deposits. In *Debris-flow hazards and related phenomena*, Springer; 81–104.

Schürch P., Densmore A.L., Rosser N.J., McArdell B.W. (2011) Dynamic controls on erosion and deposition on debris-flow fans. *Geology*, 39 (9), 827–830.

Schimmel A., Coviello V., Comiti F. (2021) Debris-flow velocity and volume estimations based on seismic data. *Natural Hazards and Earth System Sciences Discussions*, [preprint]. https://doi.org/10.5194/nhess-2020-411, in review.

Scotto di Santolo A., Pellegrino A.M., Evangelista A. (2010) Experimental study on the rheological behaviour of debris flow. *Natural Hazards and Earth System Sciences*, 10(12), 2507–2514.

Simoni A., Bernard M., Berti M., Boreggio M., Lanzoni S., Stancanelli L.M., Gregoretti C. (2020) Runoff-generated debris flows: Observation of initiation conditions and erosion–deposition dynamics along the channel at cancia (eastern italian alps). *Earth Surface Processes and Landforms*, 45(14), 3556–3571.

Stock J., Dietrich W.E. (2003) Valley incision by debris flows: Evidence of a topographic signature. *Water Resources Research*, 39(4), 1089.

Stock J.D., Dietrich W.E. (2006) Erosion of steepland valleys by debris flows. *Geological Society of America Bulletin*, 118(9-10), 1125–1148.

Takahashi T. (1978) Mechanical characteristics of debris flow. *Journal of the Hydraulics Division*, 104(8), 1153–1169.

Takahashi T. (1981) Debris flow. *Annual review of fluid mechanics*, 13(1), 57–77.

Theule J.I., Liébault F., Laigle D., Loye A., Jaboyedoff M. (2015) Channel scour and fill by debris flows and bedload transport. *Geomorphology*, 243, 92–105.

Thomas D.G. (1965) Transport characteristics of suspension: Viii. a note on the viscosity of newtonian suspensions of uniform spherical particles. *Journal of Colloid Science*, 20(3), 267–277.

Vallance J.W., Savage S.B. (2000) Particle segregation in granular flows down chutes. In *Iutam symposium on segregation in granular flows*, Springer; 31–51.

Wang B., Li Y., Liu D., Liu J. (2018) Debris flow density determined by grain composition. *Landslides*, 15(6), 1205–1213.

Yong L., Xiaojun Z., Pengcheng S., Yingde K., Jingjing L. (2013) A scaling distribution for grain composition of debris flow. *Geomorphology*, 192, 30–42.

Zheng H., Shi Z., Yu S., Fan X., Hanley K.J., Feng S. (2021) Erosion mechanisms of debris flow on the sediment bed. *Water Resources Research*, 57(12), e2021WR030707.

SUPPORTING INFORMATION

Additional supporting information may be found in the online version of the article at the publisher's website.

How to cite this article: Roelofs, L., Colucci, P., T. de Haas (2022) How debris-flow composition affects bed erosion quantity and mechanisms: An experimental assessment. *Earth Surface Processes and Landforms*, 47(8), 2151–2169. Available from: https://doi.org/10.1002/esp.5369